ISSP

Activity Report B 2001

Contents

Cover photo: The cubic anvil apparatus to produce high pressure up to 10 GPa provides multiple extrme conditions combined with low temperature and high magnetic field (top). The apparatus for electromagnetic flux-compression to produce high magnetic field over 600 tesla (bottom).

PREFACE

- Activity Report B -

ISSP was established in 1957 based on the recommendation of the National Council of Japan to promote the cooperative research throughout the country in condensed matter physics in close contact with other related fields of science such as chemistry and earth science on one hand and to pursue its own scientific research on the other hand. This foreseeing philosophy of the founders together with the constant efforts afterwards had made ISSP very active in both ways in recent years, especially after the introduction of the large group systems in 1980 and the moving to the new campus of Kashiwa. So far there were various forms of the publications to make the status of the research activity of ISSP public. New forms are now introduced; the Activity Reports A and B, which show the up-to-date status of these scientific activities in separate ways depending on the styles of the pursuing the research. This Activity Report B is based on the joint research programs conducted by ISSP in the fiscal year of 2001. In the first half of this Report the highlights are collected, whereas in the latter half all of the publications under this program are listed together with titles of the joint research programs and ISSP workshop. Those results of the joint research programs making use of the big facilities in Sychrotron Radiation Laboratory, the Neutron Scattering Laboratory and the Supercomputer Center are reported separately as their own activity reports.

We are happy to receive any comments on these Reports for the possible improvement of the overall research activity of ISSP.

August 19, 2002

Hidetoshi Fukuyama

Director
Institute for Solid State Physics
The University of Tokyo

Highlights of Joint Research

In the fiscal year of 2001, the new light source project was promoted extensively. Synchrotron Radiation Laboratory (SRL) re-designed the accelerator to be supported by as many users as possible. The accelerator design review committee has discussed the new design and the applicability of the light source from both viewpoints of synchrotron radiation users and accelerator scientists. The results of the discussion were applied to the modification of the design, and now SRL proposes a 1.8 GeV electron storage ring with 12 insertion devices optimised in EUV and SX region as the future synchrotron light source in Japan. Nation-wide synchrotron radiation related scientists support the new light source. The staff members of SRL continue the research and developments of the light source, beamlines and monochromators. The SRL is carrying out research works of the accelerator physics and developing the accelerator-related technology, many of which will be directly applied to the new light source.

On the other hand, the SRL has a branch laboratory in the High Energy Accelerator Research Organization (KEK) at Tsukuba. The branch laboratory maintains an undulator called Revolver, two beamlines and three experimental stations for angle-resolved photoelectron spectroscopy (BL-18A), spin- and angle-resolved photoelectron spectroscopy (19A) and soft X-ray emission spectroscopy (19B). They are installed in the Photon Factory (PF) and fully opened to outside users. The SRL staffs not only serve the outside users with technical support and advices, but also carry out their own research works on advanced solid state spectroscopy as well as instrumentation. In the fiscal year of 2001, the operation time of the beamlines was more than 5000 hours and the number of the users was more than 200. The main scientific interests and activities in the SRL at KEK-PF are directed to the electronic structures of new materials with new transport and optical properties. The electronic structures of solid surfaces and interfaces are also intensively studied.

The scientific highlights of the beamlines achieved in 2001 are found in the studies of the electronic structures of a novel ferromagnetic semiconductor $ZnGeP_2$:Mn observed by photoelectron spectroscopy, of the time-resolved core level photoluminescence from quantum well states of ZnSe and ZnSe/ZnCdSe/ZnSe and of the micro-domain structure observation in anti-ferromagnetic materials by photoelectron microscopy utilizing magnetic linear dichroism.

Neutron Scattering Laboratony

Since 1961, the ISSP has been playing a central role in neutron scattering activities in Japan not only by performing its own research programs but also by providing a general user program for the university-owned various neutron scattering spectrometers installed at research reactors of JAERI (Tokai). By spending 5 years starting from 1988, the ISSP constructed total 8.5 highly-sophisticated spectrometers both in a reactor hall and in a guide hall of the refurbished JRR-3M reactor (20MW) with cold source. In addition, Tohoku University owns 3.5 spectrometers and Kyoto University 1; therefore, totally 13 spectrometers belong to the university while JAERI has 9. In order to fully utilize these facilities, the previous Neutron Scattering Division of ISSP at Tokyo was promoted to the present Neutron Scattering Laboratory at Tokai in 1993. Since then, close to 300 proposals are submitted for the ISSP general user program for neutron scattering research each year, and a number of users under this program reaches over 7,000 (person-day/year). Major research areas are solid state physics (strongly correlated electron systems, high Tc superconductors, heavy fermion systems, low dimensional magnetism, high-pressure physics atc.), fundamental physics and neutron beam optics, polymer, chemistry, biolgy, and materials sciences.

Triple axis spectrometers and a high resolution powder diffractometer were utilized for a conventional solid state physics and a variety of research fields on hard-condensed matter, while in the field of soft-condensed matter physics, researches were mostly carried out by using the small angle neutron scattering (SANS-U) and/or neutron spin echo (NSE) facilities. In the fiscal year of 2001, the research topics on the hard-condensed matter science cover stripe order in high-Tc superconductors, and closely related 2 dimensional systems, charge and orbital ordering in CMR manganites, quadrapolar ordering in rare-earth based intermetalic compounds, spin dynamics of low dimensional dimer systems, etc. The research topics covered structure characterization of polymer blends, micelles, amphiphilic polymers, block copolymers, liquid crystals, proteins, inorganic gels, dynamics of brush-polymers on surface, slow dynamics of surfactants, pressure dependence of dynamics of amphiphilic membranes, and so on. The details of individual studies are reported in the NSL - ISSP Activity Report 2002.

Supercomputer Center

Supercomputer System: The main system in the Supercomputer Center of the institute (SCC-ISSP) consists of two supercomputers. Hitachi SR8000/60, called System-A, is a distributed-memory-type parallel supercomputer with 60 nodes and 640GB memory in total. Each node consists of 8 microprocessors which share their memory inside the node. Each node is optimized for vector-type large-scale calculations and archives 12GFlops peak performance.These nodes are interconnected by the multidimensional crossbar network.

On the other hand, SGI Origin 2800/384, called System-B, is a massively parallel supercomputer and consists of three hosts interconnected by high-speed GSN network. Each host is a distributed-shared-memory-type computer and equipped with 128 MIPS R12000 CPU's and 64GB memory.

User Program: The system is placed at the service of general researchers of condensed matter physics through the User Program. A project(s) can be proposed by any staff in universities or public research institutes in Japan. In order to run smoothly the User Program, the Materials Design and Characterization Laboratory (MDCL) of the ISSP has organized the Steering Committee of the MDCL, the Steering Committee of the SCC-ISSP, under which the Supercomputer Project Advisory Committee is formed to review proposals. More than half of the members of each committee are those in other institutions than the ISSP. The number of projects, the total points applied and approved in this year are listed on Table 1.

Results: The research projects carried out on the system cover various fields in the condensed matter physics. They are roughly classified into the following three:

First-Principles Calculation of Materials Properties (39, 126)

Strongly Correlated Quantum Systems (51, 275)

Cooperative Phenomena in Complex, Macroscopic Systems (18,53)

Here the first and second numbers in the parenthesis are those respectively of the projects and the publications which were reported from the project leaders. All the three involve both methodology of computation and its applications. The results of all the projects are reported in 'Activity Report 2001' of the SCC-ISSP where the following four invited articles are included in this year:

"First-Principles Study of CO and NO Absorption at Transition-Metal Surfaces" by Hideaki Aizawa and Shinji Tsuneyuki, "Strongly Correlated Electrons Studied by Path Integral Renormalization Group Method" by Masatoshi Imada, "New Type of Ordered States in Quantum Spin Systems and Their Dynamical Properties" by Seiji Miyashita, " Application of New Monte Carlo Algorithms to Various Spin Systems" by Yutaka Okabe, Yusuke Tomita and Chiaki Yamaguchi.

Table 1:Research projects approved in 2001

Class	Max.Point	Application	#of Proj.	Total points			
				Applied		Approved	
				Sys-A	Sys-B	Sys-A	Sys-B
A	100k	any time	2	200k	0	200k	0
B	2M	twice a year	53	73.5M	24.55M	73.5M	23.85M
C	20M	twice a year	67	655.1M	423.9M	561.1M	348.6M
D	none	any time	15	86.8M	389.2M	80M	373.2M
S	> 20M	twice a year	1	45M	35M	36M	28M

For System-A 1 k point corresponds to charge for CPU time of about 0.43hours by one processing element, while the corresponding figure is 2.32 hours for System-B.

Low Temperature Magnetization Study on the Spin Ice State of the Pyrochlore Oxides

K. Matsuhira and T. Sakakibara

In the pyrochlore oxide $Dy_2Ti_2O_7$ where spins are residing on the vertices of the corner-shared tetrahedra, ferromagnetic interactions and Ising anisotropy along the local <111> axes lead to a strong frustration. Accordingly, the local spin arrangement of two spins pointing outward and two spins inwards (so-called 'two-in two-out' state) is stabilized in a basic tetrahedron. For every tetrahedron, there are thus six possible combinations of spins under the two-in two-out rule. The ground state is therefore highly degenerate and a static disordered state (so-called "spin ice" state) is formed below 1 K in spite of chemically ordered system [1].

Magnetic field breaks the ground state degeneracy. Monte Carlo simulations show that the degeneracy breaking becomes a two-stage process for *H*//[111] and a magnetization plateau should appear in the intermediate fields [2]. We have examined the DC magnetization process of $Dy_2Ti_2O_7$ in magnetic fields applied along the [111] direction, using a capacitive Faraday magnetometer installed in a ^{3}He cryostat.

Figure 1 shows the results. At T = 1.65 K, the magnetization is a gradual function of field with a weak feature at around 1 T, and saturates at higher fields to the value ~5 μ_B/Dy. This moment value corresponds to the fully saturated one-in three-out (or three-in one-out) state of the Ising pyrochlore lattice with the local Ising axis pointing along the <111> directions.

On cooling below 1 K, the feature at ~1 T becomes sharper, and eventually turns into a metamagnetic step at ~0.5 K with a preceding magnetization plateau below ~0.9 T. The magnetic moment of the plateau is very close to the value 3.33 μ_B/Dy, expected for the saturated moment along the [111] direction without destroying the two-in two-out state. Clearly, the metamagnetic step near 1 T corresponds to a breaking of the spin ice state by a magnetic field strong enough to overcome the magnetic interactions, as predicted by the Monte Carlo simulations.

In the previous magnetization measurements done at 1.8 K, only a broad feature had been observed at around 1 T[3].

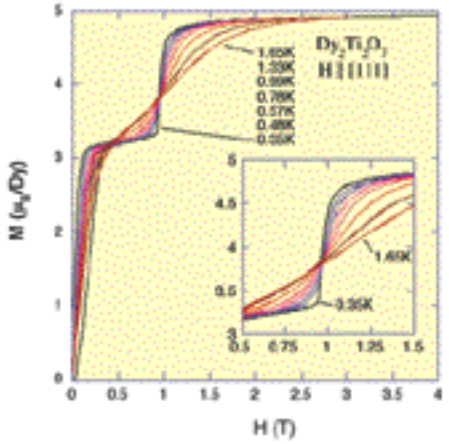

Fig. 1. Magnetization process of $Dy_2Ti_2O_7$ in magnetic fields applied along the [111] direction.At low temperatures below 1 K, a magnetization plateau develops in the field range of 0.4 ~ 0.9 T where the ice rule 2-in 2-out state is maintained. The metamagnetic step at around 1 T corresponds to a breaking of the ice rule state. The inset shows the details at around 1 T.

Our data are the first results in the low temperature regime where the ice rule configuration is well developed. Magnetization measurements at still lower temperatures are in progress.

References

[1] A.P. Ramirez, A, Hayashi, R.J. Cava, R. Siddharthan and B.S. Shastry, Nature **399** 333 (1999).

[2] M.J. Harris, S.T. Bramwell, P.C.W. Holdsworth and J.D.M. Champion, Phys. Rev. Lett. **81** 4496 (1998).

[3] H. Fukazawa, R.G. Melko, R. Higashinaka, Y. Maeno and M.J.P. Gingras, Phys. Rev. B **65** 054410 (2002).

Authors

K. Matsuhira[a], Z. Hiroi, T. Tayama and T. Sakakibara

[a]Department of Electronics, Faculty of Engineering, Kyushu Institute of Technology.

Magnetic Circular Dichroism in Ce $L_{2,3}$-Absorption Edges of Mixed Valence Compound $CeFe_2$

I. Harada and K. Kotani

Mixed valence property in Ce compounds is one of the most striking and interesting phenomena in condensed matter physics, caused by the mixing of localized states with strong correlation and itinerant states. The decomposition of the total electronic density of states into various contributions of each element and each shell would be a significant progress in understanding such a mechanism.

The recent experimental development of the X-ray Absorption Spectroscopy (XAS), $I^+(\omega) + I^-(\omega)$, and the magnetic counterpart, the Magnetic Circular Dichroism (MCD), $I^+(\omega) - I^-(\omega)$, (see Figure 1), together with the development of new generation synchrotron radiation facilities with high photon flux enable us to obtain such detailed information on electronic and magnetic states of selected atoms and of selected shells.

Let us consider a mixed valence intermetallic compound, $CeFe_2$, which behaves as a ferromagnetic material but has anomalously small magnetic moment and very low Curie temperature compared to other RFe_2 (R = rare earth).We attribute the anomaly to the mixed valence electronic state of Ce, which can be described by an impurity Anderson model[1] where the three electronic configurations, $4f^0$, $4f^1\underline{L}$ and $4f^2\underline{L}^2$, $\underline{L}$ being a ligand hole in the spin polarized 3d band of surrounding irons, are considered. In order to treat the band nature of the Fe 3d states as well as of the Ce 5d states, we adopt a cluster approach, where the hybridization between them is taken into account. This effect is the origin of the spin polarization of the 5d states and crucial for MCD

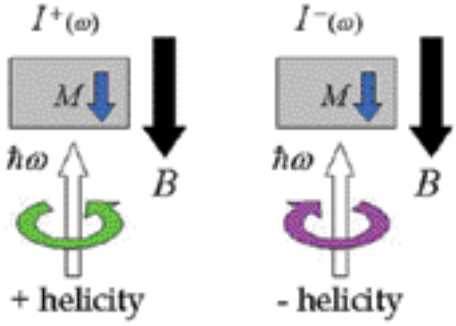

Fig. 1. Definition of the intensities, $I^+(\omega)$ and $I^-(\omega)$.

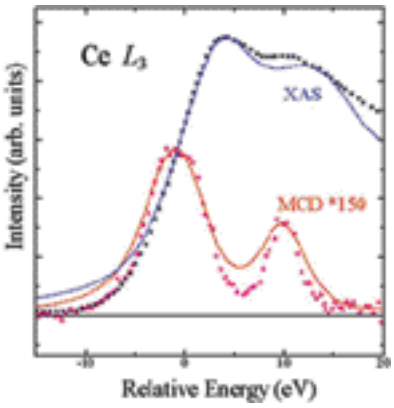

Fig. 2. XAS and MCD spectra for $CeFe_2$. The solid curves are the calculated results while the crosses and the solid circles are the experimental ones [2].

at the Ce $L_{2,3}$ edges.

Based on this model, we calculate numerically XAS and MCD spectra, which are compared quantitatively with those observed experimentally [2] in Figure 2. Then, we find the following [3]: (i)XAS shows two peaks which correspond to the $4f^0$ and $4f^1\underline{L}$ states, the $4f^2\underline{L}^2$ state overlaps with the latter. The intensity ratio of these yields the degree of the mixing of these configurations and the positions depend mainly on the core hole potential and the Coulomb interaction within the 4f states.(ii)MCD spectrum shows also two peaks but the peak positions are different from those of XAS. We attribute the difference as a consequence of the fact that the spin polarization of the 5d states depends on energy and occurs only near the Fermi energy. The anomalous magnetic properties are also naturally explainable with this model.

In conclusion, we show that the calculation based on the impurity Anderson model combined with a cluster model is appropriate for taking the Coulomb interaction and the hybridization effect into account and gives a correct interpretation for the MCD spectra at the Ce $L_{2,3}$ edges of $CeFe_2$, which gives rise to the detailed information on the characteristic electronic and magnetic states of Ce.

References
[1] For instance, see a review, A. Kotani et al., Adv. Phys. **37**, 37 (1988).
[2] C. Giorgetti *et al*., Phys. Rev. **B 48**, 12732 (1993).
[3] H. Ogasawara *et al*., J. Phys. Chemi. Solids. **63**, 1487 (2002)

Authors
I. Harada[a], K. Asakura[a], H. Ogasawara, K. Fukui[b], and A. Kotani
[a]Okayama University., [b]RIKEN/SPring-8

Quantum Transport in Transition Metal Oxides

H. Koizumi and Y. Takada

Anomalous transport properties in transition metal oxides have been a focus of attention in condensed matter physics since the discovery of high-T_c superconducting materials in cuprates. In these compounds, low-lying excited states are mostly governed by spin degrees of freedom and there are indications to show that the ground state must be a non-Fermi liquid due to strong correlation. Another aspect of the transition-metal oxides, in particular in manganese and ruthenium oxides, is that they are equipped with orbital degrees of freedom; thus, the total internal degrees of freedom consist of both spin and orbital degrees.

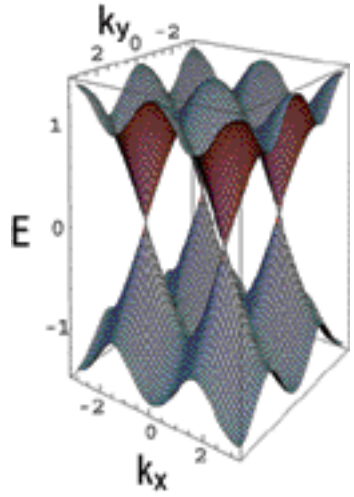

Fig. 1. Conically intersecting bands for the flux state in the 2D Hubbard model [1]. The conical intersections are located at $(\pm\pi/2, \pm\pi/2)$. They are the sources of a gauge potential A_{nk}. Its time-dependence, which may be produced by an adiabatic deformation of the lattice, is predicted to produce a *geometric phase current* in our paper [4].

In this situation, electronic motion is far from trivial due to complexity of the band dispersion curves even in a simple picture of the band electron; there are numerous crossings and also sensitively affected with spatial arrangements of the internal degrees of freedom, which is very likely to be coupled with lattice distortions through vibronic effects. Even in the cuprate case, the spin band is not simple; on the contrary, one with non-trivial flux is speculated for a certain range of parameters [1].

In order to understand the anomalous current in transition-metal compounds from a viewpoint of the band theory, we have recently reinvestigated the velocity formula for Bloch electrons. Usually the formula is given by $\partial\varepsilon_n(k)/\hbar\partial k$ as is derived in textbooks. In magnetic materials, however, it has been known that it is not valid; instead, a fictitious magnetic field $\mathbf{B}_{nk}$ has to be included:

$$\frac{1}{\hbar}\frac{\partial\varepsilon_n(\mathbf{k})}{\partial\mathbf{k}} - \dot{\mathbf{k}}\times\mathbf{B}_{nk},$$

$$\mathbf{B}_{nk} = \nabla\times\mathbf{A}_{nk};\ \mathbf{A}_{nk} = i\langle u_{nk}|\frac{\partial}{\partial\mathbf{k}}|u_{nk}\rangle,$$

where $\mathbf{A}_{nk}$ is the gauge potential (Berry phase connection) associated with the Bloch electron[2], giving rise to non-trivial geometric phase effects when the crossings of bands exist, or when either time-reversal or inversion symmetry is broken[3].

According to our recent reinvestigation [4], the above formula has to be further modified; an additional term is found in the fundamental expression for the electron velocity. By employing a path-integral representation for the propagator of a Bloch electron, the formula is obtained as.

$$\frac{1}{\hbar}\frac{\partial\varepsilon_n(\mathbf{k})}{\partial\mathbf{k}} - \mathbf{E}_{nk} - \dot{\mathbf{k}}\times\mathbf{B}_{nk};\ \mathbf{E}_{nk} = -\frac{\partial\mathbf{A}_{nk}}{\partial t}.$$

In developing the conventional Fermi-liquid theory, the second and third terms (*Geometric phase current*) in this velocity formula are not usually taken into account. Thus a further work is called for to elucidate the consequence of these terms, especially in the transition-metal compounds. Note that the second term, which is produced by the fictitious electric field $\mathbf{E}_{nk}$, explains the adiabatic charge trans-

port processes, which may be relevant in explaining the recently observed anomalous acoustoelectric effect in the film of $La_{0.67}Ca_{0.33}MnO_3$[5].

References
[1] I. Affleck and J. B. Marston, Phys. Rev. B **37**, 3774 (1988).
[2] J. Zak, Phys. Rev. Lett. **62**, 2747 (1989).
[3] M. -C. Chang and Q. Niu, Phys. Rev. Lett. **75**, 1348 (1995).
[4] H. Koizumi and Y. Takada, Phys. Rev. B **65**, 153104 (2002).
[5] Y. Ilisavskii et al., Phys. Rev. Lett. **87**, 146602 (2001).

Authors
H. Koizumi[a] and Y. Takada
[a]Faculty of Science, Himeji Institute of Technology.

First-principles Computational study of stable Adsorption sites and Dynamics for Silver adatom on Ge(001) Surface

A. Ishii and F. Komori

The determination of adsorption site of adatom is very important to consider the dynamics of adatom on surfaces. For the growth of novel and functional nano-structure on surface, the detailed dynamics is significant to recover the self-assemble mechanism.

Silver is suitable atomic specie for nano-wire because of the high conductivity. Especially, silver on clean Ge(001) surface is attractive because of the discovery of their super-conductivity below 2 K. However, silver on clean Ge(001) does not have 1ML ordered structure; the growth islands of silver on Ge(001) has usually up to thirty atoms. The reason of the lacking of the ordered structure is considered to be the large lattice mismatch. Neverthless, the determination of the atomic structure is significant to discuss the superconductivity of this system.

Komori *et al.* [1,2]observed the sereral adsorption site for silver adatom on Ge(001) surface using low temperature STM at temperatures between 65 K to RT. They distinguished the adsorption sites of Ag into several types. According to our first principle calculations, we obtain the potential surface for Ag adatom on clean Ge(001) surface. The contour map of the potential surface is shown in Figure 1. The most stable position for Ag adatom is between the dimer rows.

Our calculation shows that the two Ag adatoms are dimerized to be more stable than the individual adsorption. The calculated STM image of the Ag dimer is shown in Figure 2. This image is very similar to the STM observation

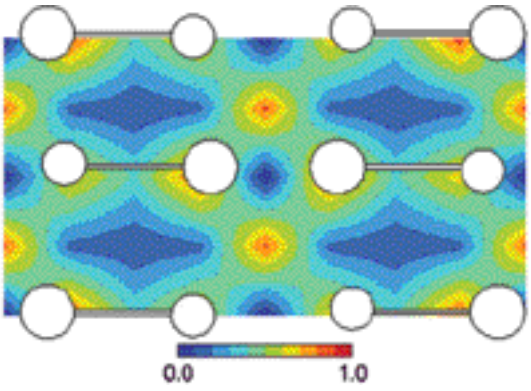

Fig. 1. Calculated potential energy surface for Ag adatom on Ge(001) c(4×2) surface. Blue area corresponds to the stable area for Ag adatom.

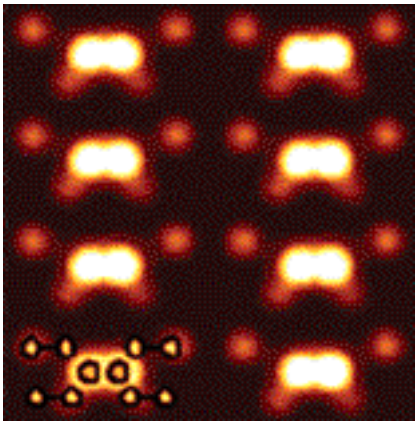

Fig. 2. Calculated STM image for Ag adatom between the Ge dimer rows on Ge(001) c(4×~2) surface. The brighter protrusions correspond to the Ag dimers.

named B1 observed by Naito *et. al.*[1] As we see in Figure 2, we found that the most of all calculated STM images are very close to the real atomic configuration. The hopping motion of adsorbed Ag adatoms was observed using STM by Naitoh et.al.[2] They distinguish the single Ag adatom into at least two types, A1 and A2 in which the both sites are placed between the Ge dimer rows. They found that the Ag adatom of A1 site cannot move at 80 K but the Ag of A2 site can move at low temperature. According to our calculation, the hopping barrier energy for the Ag adatom of the A2 site along the dimer row direction is 0.3eV, which is very close to the value determined experimentally, 0.2eV.

The A1 site is considered to be the substitutional site. Ag adatom of the substitutional site is placed at the backbond of the Ge dimer. Since the Ag adatom is usually very bright in STM images, the A1 site would be the Ag of the substitutional site. The calculated hopping barrier energy for the Ag atom of the substitutional site is 1.1 eV, which is enough value not to move at 80K.

References
[1] Y. Naitoh, K. Nakatsuji and F. Komori: Surfaces, to be published in Surf. Sci. **513** (2002) 1.
[2] Y. Naitoh, K. Nakatsuji and F. Komori: to be published in J. Chem. Phys. **117** (2002) 2832.

Authors
Akira Ishii[a] and Kaori Seino[a]
[a]Department of Applied Mathematics and Physics, Tottori University

Cyclotron Resonance of GaN/$Al_{0.13}Ga_{0.87}N$ and $In_{0.20}Ga_{0.80}N/In_{0.02}Ga_{0.98}N$ QWs Using Ultra High Magnetic Field

Y. Arakawa and N. Miura

1. Introduction

Gallium nitride and its compounds are the most promising materials for short wavelength light emitting devices and for high frequency, high power, high temperature operation transistor. In recent years significant progress has been achieved in the fabrication of optical and electronic devices based on these materials. However, the physical properties of III-V nitride materials are not well-known up to now, especially the effective mass of electron. A few cyclotron resonance (CR) experiments of AlGaN/GaN heterotructure were reported at low magnetic field [1] and none of InGaN QWs have been reported, which is due to extremely low

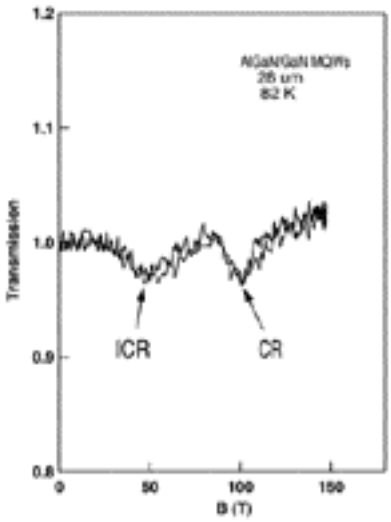

Fig. 1. The magnetotransmission spectra of GaN QWs at a wavelength of 28 μm.

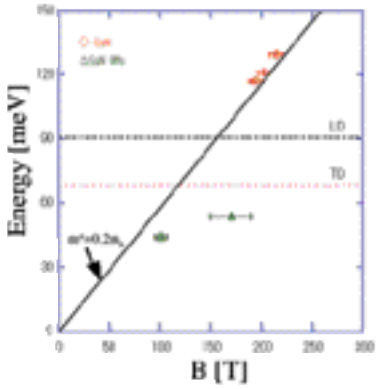

Fig. 2. Cyclotron energy versus magnetic field.

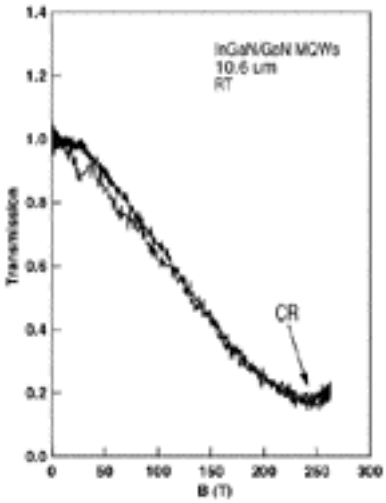

Fig. 3. The magnetotransmission spectra of InGaN QWs at a wavelength of 10.6 μm

electron mobility and large effective mass of electrons of GaN. In the present work, we used the laser lift-off (LLO) technique to remove the sapphire substrate completely and the single turn coil technique to generate ultrahigh magnetic field up to 270 T to do the CR experiment of the GaN system.

2. Experiment

The samples for this study were grown by metal organic chemical vapor deposition (MOCVD) and have structures: c-Al_2O_3/GaN (3 μm)/GaN-$Al_{0.13}Ga_{0.87}N$ (30 layers-7.3nm) or c-Al_2O_3/GaN (3 μm)/ $In_{0.20}Ga_{0.80}N$- $In_{0.02}Ga_{0.98}N$ (30 layers- 6.5nm). We have used the LLO [2] to take off the sapphire substrate and transfer sample onto KRS-5 substrate in order to carry out the CR experiment easily. Infrared laser lines at 10.6 μm, 23 μm and 28 μm were used as a radiation source. The transmission signal was detected by using the extrinsic photoconductivity of a Cu-doped Ge detector cooled to 4.2 K for a H_2O laser, and a HgCdTe photovoltaic detector cooled to 77 K for a CO_2 laser.

3. Results and discussion

Figure 1 shows a typical result of the CR experiment of GaN QWs. There is a CR peak at 101 T. From this value the CR mass is estimated as $m_{CR} = 0.264\ m_0$. Impurity cyclotron resonance (ICR) is also observed at 50 T. In Fig. 2, we plotted the dependence of the CR peak on the CR energy. The results of GaN are also plotted in the Fig. At near the TO photon energy, polaron effect becomes larger and the m_{CR} becomes heavier. Figure 3 displays the magnetotransmission of InGaN QWs subject to 10.6 μm laser radiation at 300 K. A very broad CR is observed at 240 T.

4. Conclusion

We have demonstrated the CR experiment of GaN with high-field magnetotransmission up to 270 T. A significant resonant polaron effect was observed near the TO-phonon energy.

References

[1] W.Knap et.al., App.Phys.Lett. **70**, 2123 (1997)
[2] M.K. Kelly, O. Ambacher, R. Dimitrov, R. Handschuh, and M. Stutzmann, Phys. Stat. Sol. (A) **159**, R3 (1997).

Authors
T. Q. Canh[a], S. Kato[a], K. Hoshino[a], Y. Matsuda, T.Someya[a,b], N. Miura and Y. Arakawa[a,b]
[a]Rcast, University of Tokyo, [b]ISS,University of Tokyo.

Dielectric Enhancement of Exciton Binding Energy in a Natural Quantum-Well Material

T. Kondo and N. Miura

Exciton is a quasi particle composed of an electron and a hole which are bound by the Coulomb interaction. Excitons in low-dimensional semiconductors have been an area of active research because of their unique nature and the poten-

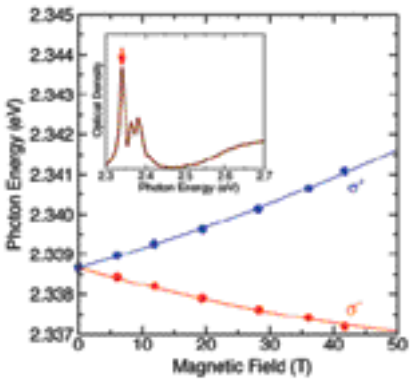

Fig. 1. Energy shift as a function of the magnetic field for the lowest 1s exciton of $(C_6H_{13}NH_3)_2PbI_4$. Circles represent the experimental results and solid lines show the theoretical fitting. Absorption spectrum is shown in the inset.

tial applications in photonics. It has been predicted that the binding energy of excitons will be substantially enhanced by the enforced Coulomb interaction in quantum wells with barrier layers of dielectric constant ε_b much lower than that of well layers ε_w. The dielectric enhancement due to electric fields penetrating into the low-ε barrier layers, however, has not been verified quantitatively to date.

A two-dimensional crystal $(C_6H_{13}NH_3)_2PbI_4$ is a natural quantum well system, in which excitons are tightly confined in the well layer of $[PbI_6]$ octahedra sandwiched between organic barrier layers. We have demonstrated that excitons in this crystal are highly stable and responsible for extremely large optical nonlinearity which can be applied to a time-to-space conversion of ultra-high bit-rate optical pulses [1]. We have quantitatively verified the exciton binding energy in $(C_6H_{13}NH_3)_2PbI_4$ is dielectrically enhanced, for the first time, in this study.

We have performed a two-photon absorption (TPA) [2], magneto-absorption (MA) and detailed reflection spectroscopies.Wannier exciton series up to $n = 4$ have been identified, and the energy separation of the discrete levels indicates that the excitons in $(C_6H_{13}NH_3)_2PbI_4$ are Wannier ones with strong two-dimensional characters. Binding energy of the lowest 1s exciton is estimated to be 350 meV. MA spectra were measured at 4.2 K in pulsed magnetic fields up to 42 T in the Faraday configuration. Diamagnetic shift clearly observed in the MA spectra of the 1s exciton (Figure) yields an important information on the dielectric environment of the excitons. The diamagnetic coefficient for a two-dimensional exciton is given by

$$c_0 = \frac{3e^{10}}{2^{11}\pi^4 \varepsilon_0^4 \varepsilon_{eff}^4 \hbar^2 E_B^3},$$

where E_B is the exciton binding energy and ε_{eff} is the effective dielectric constant the exciton feels. With the measured value of $c_0 = 2.71 \times 10^{-7}$ and $\varepsilon_B = 350$ meV, we obtained $\varepsilon_{eff} = 3.1$. This effective dielectric constant is much lower than that of the well layer ($\varepsilon_w = 6.1$) and close to that of the barrier layer ($\varepsilon_b = 2.1$). This clearly indicates that the large binding energy of the 1s exciton in $(C_6H_{13}NH_3)_2PbI_4$ is substantially enhanced by the dielectric effect.

References

[1] J. Ishi, H. Kunugita, K. Ema, T. Ban and T. Kondo, Appl. Phys. Lett. **77**, 3487 (2000).

[2] K. Tanaka, F. Sano, T. Takahasi, T. Kondo, R. Ito and K. Ema, Solid State Commun. **122**, 249 (2002).

Authors

T. Kondo[a], T. Takahashi[a], K. Tanaka[a], K. Uchida and N. Miura

[a]Department of Materials Science, The University of Tokyo

Cyclotron Resonance in Short Period III-V Semiconductor Superlattices under Ultra-High Magnetic Fields

N. Mori and N. Miura

The pioneering experiments of Esaki and Tsu [1] demonstrated the potential of the semiconductor superlattice (SL) for investigating electron dynamics in a regime not accessible in naturally occurring solids. Superlattices can be produced with SL period many times longer than the lattice constant of the host crystal. The Brillouin zone, or minizone, of the SL therefore has much smaller range of wavevector

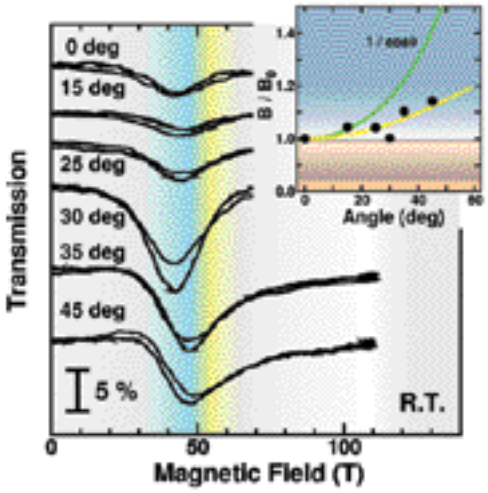

Fig. 1. Room-temperature cyclotron resonance (CR) signals of $(In_{0.2}Ga_{0.8}As)_8/(AlAs)_8$ superlattices (SL) measured with a 16.9 μm H_2O laser under a magnetic field at an angle θ to the SL axis. Inset shows θ-dependence of the normalized resonant magnetic field (closed circles). The CR positions substantially deviate from a simple cosθ-dependence (green curve).

than that for a conventional crystal. In the presence of an applied electric field along the growth direction, an electron can accelerate and move cyclically around the miniband before it undergoes a collision. A magnetic field applied perpendicular to the planes of the SL quantum wells, on the other hand, acts to quantize the in-plane motion into Landau levels. Thus the electron undergoes Bloch motion along the SL axis and cyclotron motion in the SL plane.

When a magnetic field applied at an angle θ to the SL axis, the interaction between Bloch motion and cyclotron motion occurs resulting in a complicated electronic states. Recently it has been shown that electrons in a SL under tilted magnetic fields provide an experimentally accessible non-KAM (Kolmogorov-Arnol'd-Moser) system, which is of great interest due to application in plasma physics, turbulent fluid dynamics, ion traps, and quasicrystals [2].

In the present study, we have performed cyclotron resonance (CR) measurements in short period

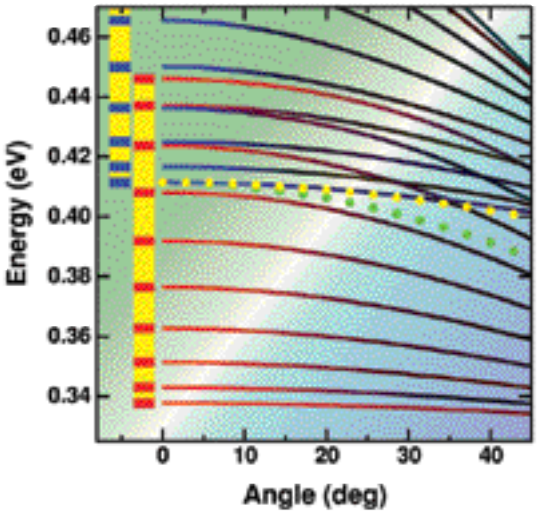

Fig. 2. Calculated energy levels in $(In_{0.2}Ga_{0.8}As)_8/(AlAs)_8$ superlattices (SL) as a function of angle θ between the magnetic field B and the normal to the SL layers. Yellow rectangle with a red (blue) striped pattern shows the lowest (first excited) Landau level miniband (LLMB) at θ = 0. The energy difference between the lowest LLMB and the first excited LLMB is consistent with the experimental findings (yellow circles, which correspond to the yellow curve in the inset of Fig. 1) and differs from a simple cosθ-dependence (green circles).

$(InGaAs)_n/(AlAs)_n$ superlattices under tilted magnetic fields to investigate Landau-level-miniband mixing.The SL samples used in the present study are $(In_{0.2}Ga_{0.8}As)_n/(AlAs)_n$ SLs grown by molecular beam epitaxy (MBE) on semi-insulating GaAs (001)-oriented substrates. 80 periods of δ-doped InGaAs/AlAs SLs are sandwiched with 10 periods undoped InGaAs/AlAs SLs. Pulsed high magnetic fields up to 150 T were produced by the single-turn coil technique. The pulsed magnetic field was applied to the samples at an angle θ between the magnetic field *B* and the normal to the SL layers.

Figure 1 shows CR signals of $(In_{0.2}Ga_{0.8}As)_8/(AlAs)_8$ superlattices, which clearly shows that the CR positions substantially deviate from a simple $\cos\theta$-dependence suggesting the Landau-level-miniband mixing. The observed CR positions are found to agree with the calculated results (Figure 2).

References

[1] L. Esaki and R. Tsu, IBM J. Res. Dev., **14**, 61 (1970).
[2] T.M. Fromhold, A.A. Krokhin, C.R. Tench, S. Bujkiewicz, P.B. Wilkinson, F.W. Sheard, and L. Eaves, Phys. Rev. Lett. **87**, 046803 (2001).

Authors

N. Mori[a], H. Momose, Y. Tujimoto, M. Itoh, and C. Hamaguchi, N. Miura

[a]Osaka University.

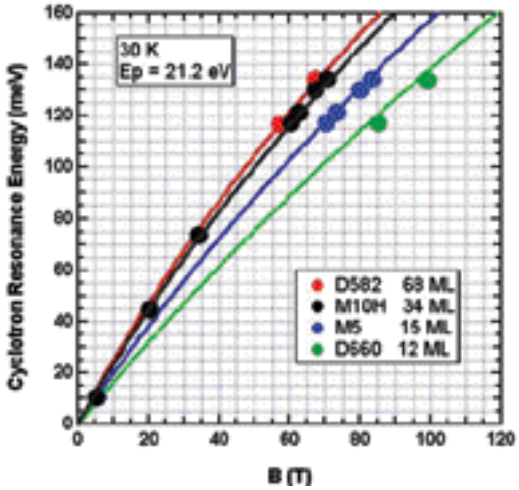

Fig. 2. Summary of measured results of cyclotron resonance (CR) showing CR energy vs. magnetic field (Solid marks; experiments, Solid lines; theoretical calculation based on band theory). As quantum well thickness or thickness of InGaAs layer decreases from 68 ML to 12 ML, CR energy decreases relatively, demonstrating the heavier electron effective mass in thinner QW. One reason of the heavier mass is the increase of eigen-energy in thinner QW. It is the evidence of electron confinement in InGaAs layer that the experiments fit well with a band theory in InGaAs QW under very high magnetic field. Even at 12 ML QW, a simple band theory assuming an infinite spread of crystals applies though the slight shift appears. This is another evidence of lattice-matching whole through the crystal structure where the averaged lattice-constant is common everywhere in barriers and wells.

Cyclotron Resonance of Confined Electrons in Semiconductor Quantum Well of Near Ten Monolayer Thickness

N. Kotera and N. Miura

Semiconductor nanometric structures called InGaAs/InAlAs quantum wells (QWs) are widely used in light-emitting diodes or lasers. The slightly-different two crystals, InGaAs as a 'well' and InAlAs as a 'barrier', are alternately grown on Indium Phosphide crystal surface. Conduction electrons in QWs are confined in a square potential well (Fig.1), comprised by InGaAs layer. Confined elecrons in QWs have one or more discrete eigen energies, if they do not liberated into the barrier by tunneling.

In the recent state-of-the-art technology, well thickness

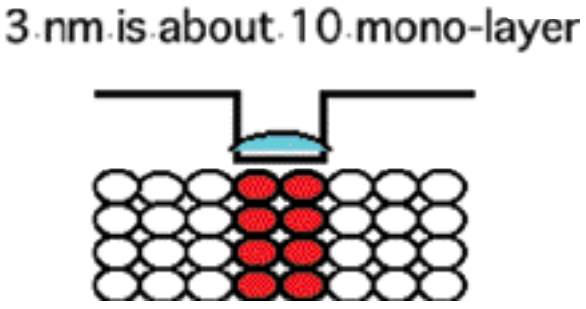

Fig. 1. Cross-sectional image of nano-scale quantum well (QW) structures utilizing slightly-different two crystals, red atoms (well region) and white ones (barrier region). Electro-static potential of square shape is illustrated where electron wave-function of free electrons is confined in a direction normal to the QW interface. Penetration of wave-function into the barrier was the problem in QW system so far. Key to solve this difficulty was to raise the barrier height. Using molecular-beam-epitaxy technique, such a fine structure was fabricated, where QW thickness was tested in a range from 12 monolayer (ML) to 68 ML. 10 ML thickness corresponds to about 3 nm in the experimental material system. Monolayer thickness was defined as an averaged distance of constituent atoms like In, Ga, and As.

can be made as thin as 10 monolayers (MLs). Ten ML thickness of equally mixed crystal of InAs (Indium Arsenide) and GaAs (Gallium Arsenide) corresponds to 3 nm in length (Fig. 1). A 'band theory' or the 'effective-mass-approximation' describing electronic states in QWs must be checked in such a thin layer.

In the popular GaAs/GaAlAs QW system, electrons tend to be free from GaAs because of the lower barrier height of 0.3 eV. Wave functions are penetrating in a direction normal to the QW interface (Fig.1).

In this experiment, however, high barrier height of 0.52 and 1.6 eV was realized by using InGaAs/InAlAs QW system (specimen names, M5 and M10H) and InGaAs/AlAsSb QW system (specimen names, D582 and D660), respectively. To generate free electrons in semiconductors impurity atom, Si, was doped in InAlAs layer (for M5 and M10H specimens) or InGaAs layer (for D582 and D660 specimens). This QW structure offered a good means to check the band theory in thin-layer semiconductor, where only one material (InGaAs) controls the electronic states because highly confined free electrons in QW were realized in this experiment. Small 'band-gap energy' of 0.8 eV in InGaAs crystal also simplified the description of electronic states, where the (8 x 8) determinant representation can be reduced to a third-order equation of energy for conduction electrons. Characteristic 'electron effective-mass' in a direction normal to the QW interface is given there by a simple algebraic equation of electron energy.

Pulse cyclotron resonance (CR) up to 100 T for these specimens was measured near 30 K by using the single-turn coil technique scanning magnetic flux density, B, under various infrared wave-lengths ranging 118.8 to 9.25 micron generated from carbon-dioxide-gas laser and methanol-vapor laser (Fig.2).

If the electron mass is a constant, CR energy changes linearly on B. If the mass increases with increasing electron energy, CR energy changes sub-linearly with B (Fig. 2). In

experiments, as the QW thickness decreases from 68 ML to 12 ML, CR energy tends to decrease (from red mark to green mark). The inverse of gradient of CR-energy-vs.-B curve reflects the magnitude of electron mass, which clearly increased in thinner QW specimen.

Theoretical calculation based on the above simple 'band theory' (solid lines in Fig. 2) fit quantitatively with experiments (marks in Fig. 2), except the slight shift at the thinnest 12 ML case. A reasonable band parameter, Ep, to fit the experiments was determined to be 21.2 eV. Wave-function confinement was thus evidenced by comparing CR experiments with a band theory in a specially tailored QW specimens. Applicability of a simple model of chracteristic electron-effective-mass called 'non-parabolic effective mass' was first demonstrated experimentally. Anisotopy of masses, mass differences in directions normal and parallel to the QW interface, will be clarified quantitatively.

References
N.Kotera, K. Shibata, T. Kawano, T. Sakai, T. Ikaida, N. Miura, N. Georgiev, T. Mozume, International Symposium on Compound Semiconductors 2001, to be published in IOP Conference Series (Tokyo, Japan, October 1-4, 2001).

Authors
N. Kotera[a] and N. Miura
[a]Kyushu instilute of technology

Magnetization Plateau in Cs_2CuBr_4

H. Tanaka and T. Goto

Cs_2CuBr_4 has an orthorhombic structure with space group Pnma. For isostructural Cs_2CuCl_4, magnetic properties have been extensively investigated by Coldea *et al.* [1] using neutron inelastic scattering technique. They demonstrated that Cs_2CuCl_4 is magnetically described as the quasi-2D distorted triangular antiferromagnet in the bc-plane as shown in Fig. 1. The ordering temperature of Cs_2CuCl_4 is $T_N = 0.62$ K. In the ordered phase, the magnetic structure is incommensurate along the *b*-direction due to $J_1 \neq J_2$. Coldea *et al.* also showed that the ordered phase vanishes before reaching the saturation for $H \parallel$ c-axis. The similar magnetic behavior is also expected in Cs_2CuBr_4. Therefore, we have performed the high field magnetization and specific heat measurements in Cs_2CuBr_4.

From the specific heat measurements, it was found that

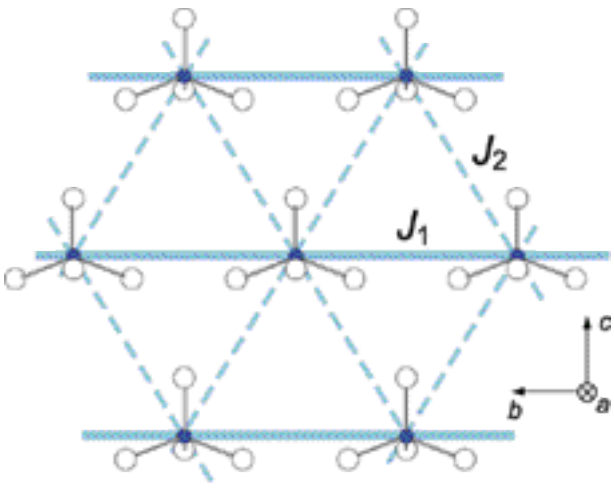

Fig. 1. Arrangement of Cu^{2+} ions in the *bc*-plane and exchange interactions in Cs_2CuCl_4 and Cs_2CuBr_4. Blue circles and open circles denote Cu^{2+} ion and Br^- ion, respectively.

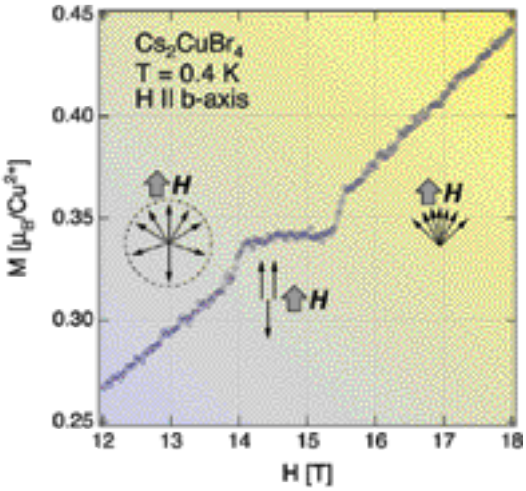

Fig. 2. Magnetization curve in Cs_2CuBr_4 for $H \parallel$ b-axis around $H = 15$ T measured at $T = 0.4$ K. Transitions between helix-uud and *uud*-fan structures are expected to occur.

Cs_2CuBr_4 undergoes magnetic ordering at $T_N = 1.4$K, which is about twice as large as that of Cs_2CuCl_4. The magnetization saturates at $H \sim 30$ T, and the saturation magnetization is slightly higher than 1 μ_B per Cu^{2+} ion. This result indicates that the orbital moment is quenched, so that the magnetic moment is approximately given by spin only. Figure 2 shows the magnetization curve around $H = 15$ T measured at $T = 0.4$ K for $H \parallel b$-axis. A magnetization plateau is clearly observed at one third of saturation magnetization M_s. The plateau was also observed for $H \parallel$ c-axis. One the other hand, the magnetization curve for $H \parallel$ a-axis is monotonical up to the saturation.

In the 2D triangular antiferromagnet, the magnetization plateau can appear at one third of M_s, where the collinear up-up-down (uud) spin structure is realized with the help of the quantum fluctuation [2]. Since the magnetic properties may be described by $S = 1/2$ quasi-2D distorted triangular antiferromagnet as shown in Fig. 1, we infer that the magnetization plateau in Cs_2CuBr_4 is attributed to the quantum fluctuation and the uud spin structure is realized at the plateau.

The transition between the slope and the plateau regions appears to be of the first order. This implies that the ordering vector **Q** varies discontinuously at the both edges of the plateau, which suggests an incommensurate-commensurate transition. The spin structure below and above the plateau region should be helical and fan structures, respectively.

Reference
[1] R. Coldea *et al.*, Phys. Rev. Lett. **86** 1335(2001) .
[2] A. V. Chubukov and D. I. Golosov, J. Phys.: Condens. Mater **3** 69 (1991) .

Authors
T. Ono[a], H. Tanaka[a], H. A. Katori[b], F. Ishikawa, Y. Mitamura and T. Goto
[a]Tokyo Institute of Technology, [b]RIKEN

Magnetization Process in Mixed Magnetic Chains $(CH_3)_2CHNH_3Cu(Cl_xBr_{1-x})_3$

I. Yamada and T. Goto

Recently, we found useful candidate compounds which consist of the gapless state induced by bond randomness, i.e.,$(CH_3)_2CHNH_3Cu(ClxBr_{1-x})_3$ (abbreviated as

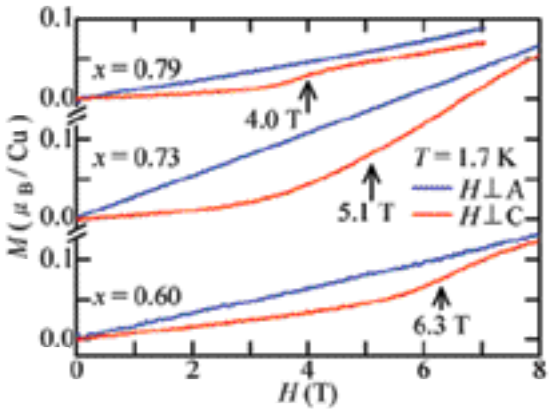

Fig. 1. The magnetization curves for x = 0.79, 0.73 and 0.60. The spin flop transition appears when $\boldsymbol{H}\perp$C plane. Each peak position of the dM/dH curve is defined as the spin flop transition field indicated by an arrow.

IPACu(Cl_xBr_{1-x})$_3$)[1] obtained by mixing the almost isomorphous compounds $(CH_3)_2CHNH_3CuCl_3$ and $(CH_3)_2CHNH_3CuBr_3$[2]. As shown in the schematic drawing of the crystal structure of $IPACuX_3$ (X = Cl, Br), which is given in Fig. 1 in Ref. **3**, the neighboring Cu ions both in each dimer and between the dimers are bibridged by X ions. From the analysis of the magnetic susceptibility $\chi(T)$ data[3], the intradimer exchange interaction J_{intra}(X, X) and the interdimer one J_{inter}(X, X) were determined to be J_{intra} (Cl, Cl)/k = + 54.1 K, J_{inter}(Cl, Cl)/k = -23.5 K, J_{intra}(Br, Br)/k =-61 K and J_{inter}(Br, Br)/k = -33 K.

When Cl ions in $IPACuCl_3$ are randomly substituted by Br ions, we expect J_{inter}(Cl, Br) = J_{inter}(Br, Cl) < 0 because of J_{inter}(Cl, Cl) < 0 and J_{inter}(Br, Br) < 0. On the other hand, J_{intra}(Cl, Br) = J_{intra}(Br, Cl) < 0 is obtained from analysis of the $\chi(T)$ data[4]. To express the degree of the bond randomness, we introduce a parameter P which indicates the probability of J_{intra}> 0. Thus, we obtain the relation P = x^2[4].

From the $\chi(T)$ and magnetic specific heat measurements for $0 \leq x \leq 1$[1], we confirmed that the antiferromagnetic long-range order occurs at $T_N \simeq$ 15 K for 0.44 < x < 0.87 because of realizing the gapless state induced by bond randomness. To obtain more information about the gapless state, we measured the magnetization process up to 41 T at 1.7 K ($\ll T_N$) for 0 < x < 1. An external field H was applied along the normals of the three orthogonal surfaces of each as-grown sample, A, B and C, as named in Ref. 3.

Figure 1 shows the representative $M(H)$ curves over the gapless state. The $M(H)$ curves for $\boldsymbol{H}\perp$A plane show a straight line, but those for $\boldsymbol{H}\perp$c plane exhibit a typical spin flop transition. Therefore, the magnetic easy axis is found to be perpendicular to the c plane. The variation of the spin flop transition field H_{sf} with x as well as P = x^2 are shown in Fig. 2.

The appearance of magnetic long-range order means that the expected value of spins is not zero, i.e., $\langle S_i^z \rangle \neq 0$. We examine how $\langle S_i^z \rangle$ is affected by changing bond randomness. On the basis of the molecular field theory, H_{sf} is represented by using $\chi_{\parallel}$ and $\chi_{\perp}$ as $H_{sf} = \sqrt{2K/(\chi_{\perp}-\chi_{\parallel})}$, in which K is the magnetic anisotropy constant. Since $K \propto \langle S_i^z \rangle \langle S_i^z \rangle$ in the present compounds, the variation in K with P suggests how $\langle S_i^z \rangle$ changes by varying the bond randomness. Applying the $\chi(T)$ data [1] into $\chi_{\parallel}$ and $\chi_{\perp}$, we calculate K at each value of χ (Fig. 2).

As can be seen in Fig. 2, K versus P describes a parabolic curve with the maximum at $P \simeq 0.5$, which indicates that $\langle S_i^z \rangle$ reaches its maximum at $P \simeq 0.5$, the point at which bond randomness is the highest.

Reference
[1] H. Manaka et al., Phys. Rev. B **63** (2001) 104408.
[2] D. R. Bloomquist and R. D. Willett, J. Am. Chem. Soc. **103** (1981) 2615.
[3] H. Manaka *et al.*, J. Phys. Soc. Jpn. **66** (1997) 564; **66** (1997) 1908.
[4] H. Manaka *et al.*, in preparation.

Authors
H. Manaka[a], I. Yamada[b], H. Mitamura[c], and T. Goto
[a]High Energy Accelerator Research Organization, [b]Chiba University
[c]Chiba University

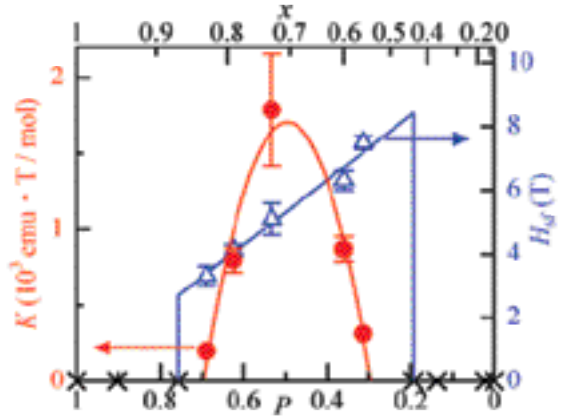

Fig. 2. The variations of the magnetic anisotropy constant K and the spin flop transition field H_{sf} with x and P=x^2, as indicated by closed circles and the open triangles, respectively. The crosses represent no observation of the spin flop transition. The solid lines are guides for the eyes.

Surface Study of Quan-tum Fluids

K. Kono and H. Ishimoto

Surface phenomena on liquid helium or quantum fluids provide a unique opportunity to study low-dimensional physics. Electrons on liquid helium, positive and negative

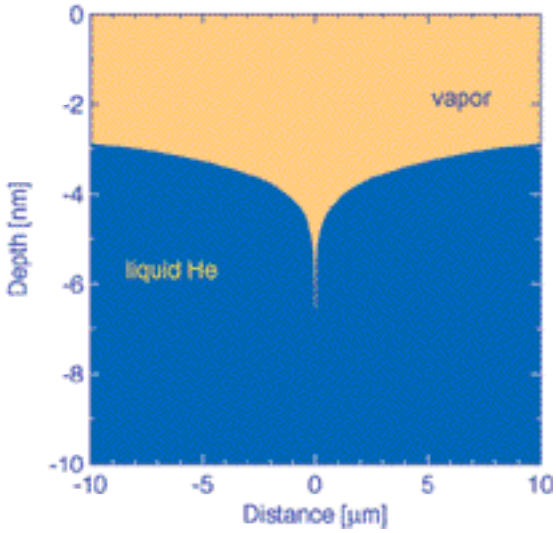

Fig. 1. Surface profile at a termination point of quantized vortex. Vortex is located vertically at distance = 0. The profile is according to Harvey and Fetter [J. Low Temp. Phys. **11** (1973) 473.]

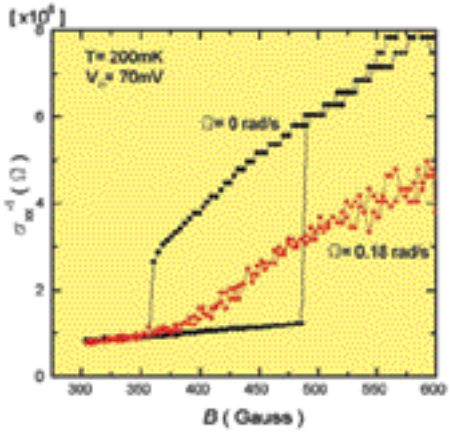

fig. 2. Magneto resistance of the Wigner crystal as a function of the magnetic field. The rotation of the cryostat smears out the sharp transition due to the decoupling from the coupled phono ripplon mode.

ions under the free surface of liquid helium, and hydrogen atoms adsorbed on the surface are examples of such unique low-dimensional systems. The important advantage in studying these systems is cleanliness and well-defined characteristics. In particular, helium-3 provides the purest surface. Here, we describe recent experimental achievement of the magneto-conductivity measurement of the Wigner solid on a rotating superfluid helium-4 surface. Two-dimensional electrons on a liquid helium surface form the Wigner solid at sufficiently low temperatures. The formation of the Wigner solid inhibits the fast diffusion of electrons on the helium surface and accordingly the electron stays at its lattice site long enough time to produce dimples on the liquid helium surface. The dimples are produced commensurately with the Wigner solid and so it is called the dimple lattice.The dimple lattice results in a prominent influence on the transport properties of the Wigner solid.Since the motion of the Wigner solid is accompanied with the dimple motion, electrons become less mobile in the Wigner solid phase. The dynamical sliding phenomena can be observed by applying the magnetic field perpendicular to the surface under the concentric Corbino geometry. When the driving electric field, which is oriented in the radial direction, is strong enough, the Wigner solid starts to leave the dimple lattice and to move in the azimuthal direction. The transition is cooperative because of the strong correlation between electrons. Because the substrate for the Wigner solid is liquid helium, the system is so homogeneous that it is extremely suitable to study such a cooperative dynamic transition. Conversely, however, it is difficult to introduce inhomogeneous pinning of the Wigner solid in this system. In order to overcome this restriction and expand the research possibility to the inhomogeneous sliding, we develop the idea to utilize termination points of quantized vortices at the free surface as pinning centers for the Wigner solid.

Fig. 1 shows the surface profile at the termination point of the vortex, where the free surface produces a sharp dip of about 7 nm deep, with a wide depressed surrounding area.It may be an interesting problem to consider how 2D electrons are scattered, trapped, and localized because of such dips, in particular, in the presence of perpendicular magnetic field. So far, no theoretical treatment has been carried out on the problem. Experiment has been carried out using a special dilution refrigerator equiped with tandem sorption pumps with which He^3 is circulated only in the cryostat. The dilution is mounted on a rotating turn table to produce the quantized vortices in superfluid helium-4. The detailed description of the apparatus is given elsewhere.

Fig. 2 shows the magneto-resistance of the Wigner solid with and without vortices. Significant influence from the vortices has been observed for the first time.Without vortices the transition to the sliding state from the coupled state is very abrupt and with hysteresis, whereas under rotation the transition becomes gradual and without hysteresis. This behavior may suggest the inhomogeneous transition between two states. Therefore, the role of the dips at termination points of vortices is not so simple to act as pinning centers. By looking at the overall landscape of the surface profile, one is aware that the profile has both a very sharp central dip and long range gradual tail part. The motion of electrons under the influence of such an unusual potential should shed a new light on the physics of 2-dimensional electrons on the liquid helium surface.

Principal publication and Author
K. Kono
Affiliation: RIKEN, Hirosawa 2-1, Wako-shi, 351-0198 Japan

Vortex Nucleation and Texture of Rotating ^{3}He-A in Narrow Cylinders

T. Mizusaki and M. Kubota

Helium is a rather simple atom, which consists of nucleus made of two protons and either one (^{3}He) or two (^{4}He) neutrons(s). Although chemical properties as well as high temperature physical properties are quite the same for ^{3}He and ^{4}He, drastic difference appears as to the superfluid properties. ^{4}He undergoes into superfluid at T_λ = 2.17 K (at saturated vapor pressure, SVP) whereas ^{3}He becomes superfluid first at about 1 mK at SVP, three decades lower temperature. This is understood as that Quantum statistics of the atoms is essential for superfluid occurrence. For ^{4}He Bose Einstein Condensation is essential for the occurrence of superfluidity, whereas for Fermion system ^{3}He, BCS mechanism with p-wave Cooper pairs is responsible for superfluidity at $T_c << T_F = \sim 1K \sim T_\lambda$.

Superfluidity is studied under rotation just as study of superconductivity in magnetic field. Bulk properties of superfluid ^{3}He has been studied under rotation since some time [1], we have started new activity to study superfluid ^{3}He in restricted geometry [2]. Since the Cooper pair of ^{3}He has internal freedom with 18 components, there are plenty of possible superfluid states and bulk liquid ^{3}He displays

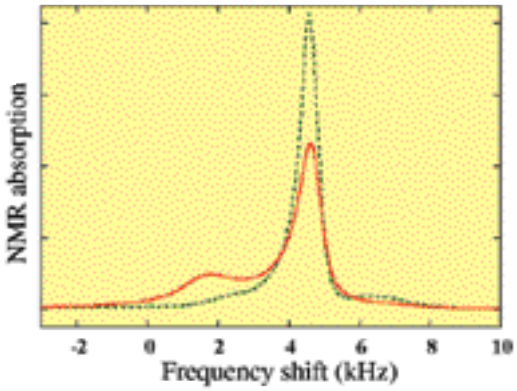

Fig. 1. NMR absorption line shapes for the 0.2mm sample at T/T_c = 0.75 as a function of frequency shift from Larmor frequency. The dotted green line was taken at rest and the solid red line was taken at rotation speed of 6.28 rad/sec.

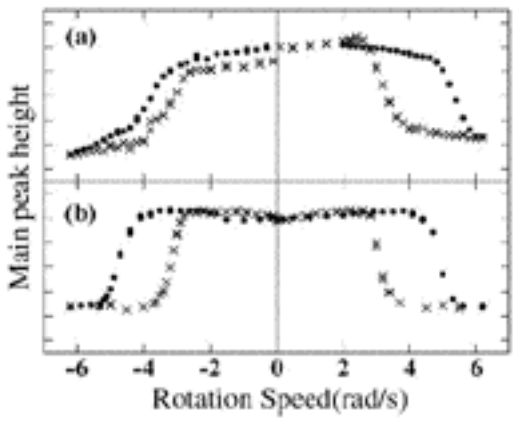

Fig. 2. Main NMR absorption peak height during acceleration (solidcircle) and deceleration (cross). (a):the sample was cooled to superfluid under rotation at rest. and (b): it was cooled under rotation of + 2rad/sec

three superfluid states, A, A1, and B phases. Quite different up to 11 types of vortices are expected in the bulk liquid and 7 of them have been reported experimentally. There is so called 'texture', which is configuration of arrangement of internal freedom, namely of l-vector and d-vector, and determined by external conditions, magnetic field, boundary, flow field, etc. The liquid in a confined geometry is expected to have quite a different configuration.

Superfluid ^{3}He-A in small cylinders has been being studied with the world fastest rotational cryostat at Kubota lab. ISSP, U-Tokyo. Since ^{3}He has nuclear spin, NMR is one of the most effective methods to study this superfluid and it is applied for the present study. Fig.1 shows typical cw-NMR absorption line shape of superfluid ^{3}He-A phase confined in 0.2mm diameter cylinders at $T/T_c = 0.75$. The main peak for the ^{3}He-A phase appears about 4.5 kHz shifted from the normal phase Larmor frequency. Under rotation above a critical angular velocity, this main peak decreases its height, instead a new peak appears at a lower frequency. The position of this new peak is characterized by a parameter R_t^2, defined by $\Delta f = R_t^2 (f_L^A)^2 / (2f_0)$, where Δf is the frequency shift from Larmor frequency f_0 and f_L^A is temperature dependent longitudinal frequency in the A phase. So the main peak position is at $R_t^2 = 1.0$, whereas the new peak position is $R_t^2 \sim 0.37$. The new peak position is very close to the doubly quantized nonsingular vortex that is observed in bulk ^{3}He-A[1].

Fig. 2 shows the change in NMR absorption signal as a function of the rotational speed Ω. Since the main peak height is most sensitive to the change of texture, it is plotted against Ω. The difference in (a) and (b) is the difference in cooling procedure, either if the system is cooled through T_c under rotation or not. This is the first observation of single vortex formation, which shows history dependent configuration. As one can see from Fig. 2 this result could be obtained only by the speed of rotation in the ISSP rotating cryostat doubling the former cryostats[1].

References

[1] O.V. Lounasmaa and E. Thuneberg, Proc. National Acad. Sci. USA **96** (1999) 7760.
[2] R. Ishiguro, M. Yamashita, T. Igarashi, E. Hayata, O. Ishikawa, Y. Sasaki, K. Fukuda, M. Kubota, H. Ishimoto, T. Mizusaki, T. Ohmi, T. Takagi, and R. E. Packard, to be published in LT23 Proceedings.
[3] M. Kubota, T. Obata, R. Ishiguro, M. Yamashita , T. Igarashi, E. Hayata, O Ishikawa, Y. Sasaki, N. Mikhin, M. Fukuda, V. Kovacik, T. Mizusaki, to be published in LT23 Proceedings.

Authors
R. Ishiguro[a], M. Yamashita[a], E.Hayata[a], T. Ohmi[a], Y. Sasaki[a], T. Mizusaki[a], K. Fukuda[b], O. Ishikawa[c], T. Takagi[d], T. Igarashi, T. Obada, M. Kubota, H. Ishimoto
[a]Dep. of Physics, Graduate School of Science, Kyoto University, [b]College of Medical Technology, Kyoto University. [c]Dep. of Physics, Osaka City University. [d]Dep. of Applied Physics, Fukui University.

Quantum Critical Phenomena in $UNiGa_5$

R. Settai and Y. Uwatoko

Recently, quantum critical phenomena induced by pressure have been investigated intensively in cerium and uranium compounds [1, 2]. As pressure P is applied to some cerium and uranium compounds with the magnetic ordering, the ordering temperature decreases and becomes zero at the critical pressure P_c. Around the critical pressure, a heavy fermion state or non-Fermi liquid behavior appears at low temperatures. Moreover, superconductivity appears in some compounds. As a candidate of such compounds, we investigated the antiferromagnet compound $UNiGa_5$ with T_N = 86 K by measuring the electrical resistivity down to 2 K under pressures up to 8.5 GPa using a BeCu piston-cylinder cell and a cubic anvil apparatus.

The electrical resistivity shows a sharp kink at T_N = 86.5 K under ambient pressure (Figure 1). T_N decreases with increasing pressure and the kink disappears above P_c = 4.5 GPa. An inset of figure 1 is the P-T phase diagram for $UNiGa_5$. Figure 2 shows the T^2 -dependence of the electrical resistivity. The Fermi liquid nature is found at 1.5 and 2.5 GPa below about 15 K. From 5.0 to 5.5 GPa, the slopes of T^2-dependence become steep, indicating an evolution of the heavy fermion state, or the electrical resistivity deviates from the T^2-dependence, reflecting the non-Fermi liquid nature. With further increasing pressure, the Fermi liquid nature fully recovers and is satisfied in a wide temperature range, as seen at 7.0 and 8.5 GPa.

Superconductivity was not found in the present experiment for $UNiGa_5$. However, the superconductivity appears below about 1 K in uranium compounds in general. Measurements under the critical pressure at much lower temperature are needed to confirm the superconductivity , together with the non-Fermi liquid behavior for $UNiGa_5$.

References

[1] N. D. Mathur *et al.*, Nature, **394**, 39 (1998).

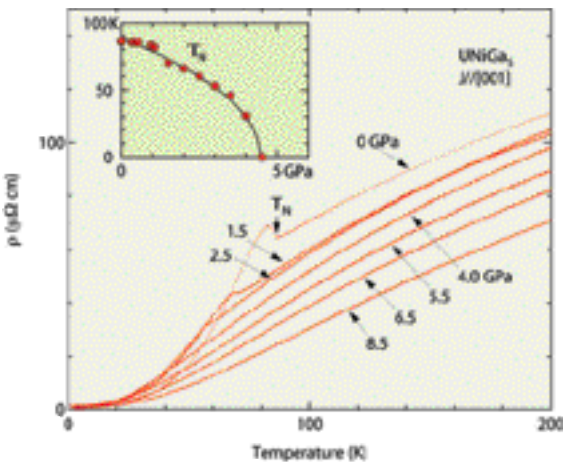

Fig. 1. Temperature dependence of the electrical resistivity under pressure in $UNiGa_5$. A kink in the resistivity corresponds to the Néel temperature. An inset is the pressure dependence of the Néel temperature. Critical pressure in $UNiGa_5$ is about 4.5 GPa.

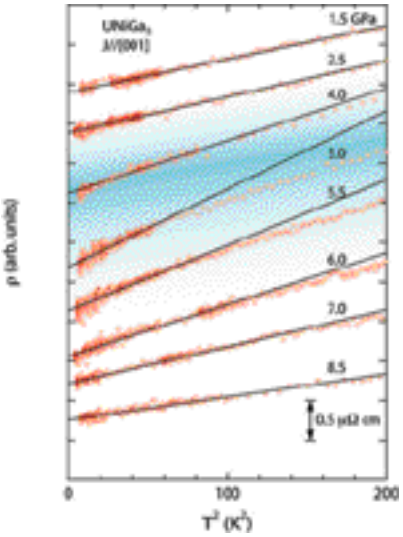

Fig. 2. T^2-dependence of the electrical resistivity under pressure in $UNiGa_5$. The slope of the T^2-dependence is steep around the critical pressure, or the electrical resistivity deviates from the T^2-dependence, reflecting the non-Fermi liquid nature.

[2] S. S. Saxena *et al.*, Nature, **406**, 587 (2000).

Authors
R. Settai[a], M. Nakashima[a], Y. Haga[b], Y. Onuki[a,b] and Y. Uwatoko
[a]Graduate School of Science, Osaka University, [b]Advanced Science Research Center, Japan Atomic Energy Research Institute.

Anomalous Magnetism of a $PrCu_2Ge_2$ Single Crystal

T. Shigeoka and T. Uwatoko

The ternary compound $PrCu_2Ge_2$, crystallizing in the tetragonal $ThCr_2Si_2$-type structure, shows interesting magnetic behaviors; It has an anomalously high Neel temperature and the existence of another magnetic transition at 4.2 K was suggested [1]. In order to elucidate this magnetic behavior, measurements of magnetic susceptibility and magnetization have been carried out on a $PrCu_2Ge_2$ single crystal compound at the Institute of Solid State Physics, University of Tokyo.

The c-axis susceptibility shows a very peculiar behavior

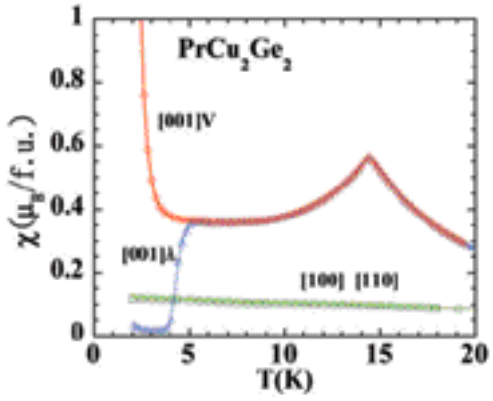

Fig.1. Temperature dependence of magnetic susceptibility along the main symmetry directions of the tetragonal cell in low temperatures on a $PrCu_2Ge_2$ single crystal compound. The red circles and blue triangles show the susceptibility along the c-axis in the virgin state and a state after saturation process, respectively. The green squares show the susceptibility in the basal plane

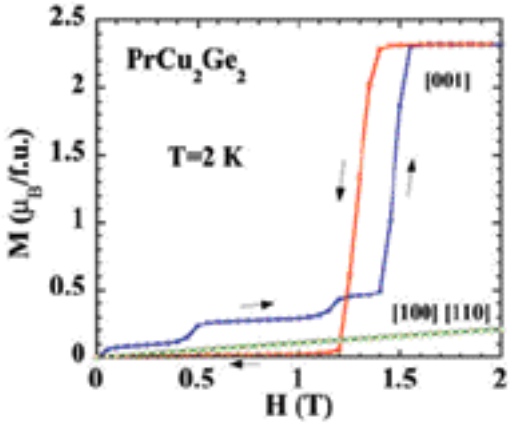

Fig. 2. Magnetization as a function of applied magnetic field along the main symmetry axes at 2 K for the $PrCu_2Ge_2$ single crystal. The blue and red curve shows an ascending and descending process along the c-axis, respectively.

(Fig. 1); the susceptibility of a virgin state is different from one after a saturation magnetization process. Below 3.5 K, a strong increase in virgin susceptibility can be observed with decreasing temperature. After the magnetization is saturated by an applied field above 1.5 T at low temperature of 2 K, the susceptibility becomes very small. Then with increasing temperature, it persists the small value below 3.5 K, increases rapidly around 4 K, reaches the value of the virgin susceptibility at 5 K and at last above 5 K, behaves similarly to one of the virgin state. This behavior suggests a magnetic transition around 4 K and the ground state may be forced to change by a saturation process.

The magnetization along the easy c-axis shows a very peculiar behavior (Fig. 2): an irreversible magnetization process; in the ascending process, a four-step metamagnetic process appears. Magnetization increases rapidly around 0.2 T, 0.45 T, 1.15 T and 1.45 T, and reaches the saturation value of 2.34 μ_B. Then in the descending process after saturation, it decreases rapidly around 1.3 T, goes across one of the ascending process and reaches a very small value below 1.2 T. This peculiar irreversible process appears only in the virgin state and has been never seen yet. The process in the second run becomes a one-step metamagnetic one similar to one of the descending process in the virgin state with small hysteresis; it becomes a reversible process. The irreversible process can be observed up to 3.5 K. Above 4 K, the process becomes a reversible one-step one. Regarding to the four-step metamagnetic process, the magnetization of each plateau is 0.09 μ_B, 0.27 μ_B, 0.45 μ_B and 2.34 μ_B, corresponding to 1/26 M_s, 3/26 M_s, 5/26 M_s and M_s (= the saturation moment), respectively. It is worth noting that the ratios have a large common denominator (= 26), suggesting a long period antiferromagnetic structure althoug a simple antiferromagnetic structure reported. And it suggests that this metamagnetic process occurs by spin-flip transitions. Though the origin of the irreversible process is unknown yet, orbital effects, quadrupolar effects may be responsible. Further study is now in progress.

References

[1] E.V. Sampathakumaran, I. Das and R. Vijayaraghavan, Solid State Commun., **83**, 609 (1992).

Authors
T. Shigeoka[a], Y. Taneda[a], M. Hedo and Y. Uwatoko
[a]Faculty of Science, Yamaguchi University.

Modulation in Electrical Conduction of Single-Wall Carbon Nanotubes in Zeolite Single Crystals by Laser Light Irradiation

N. Nagasawa and T. Suemoto

Carbon nanotubes (CNs) formed in micro-channels aligning along the C-axis of a Zeolite (AFI) single crystal have unique electrical and optical character. Tang's group has reported electrical transport properties of the AFI-CN crystal [1] as well as its superconductive character at low temperature [2].According to the analyses of the optical absorption [3] and Raman spectra [4], metallic and semiconducting tubes coexist in this system.

We have found that the electrical properties are modulated by the laser light irradiation. The modulation has been seen not only in the photo-current [5] but also in the bias current. Figure 1 shows a schematic illustration of our experimental set-up to measure the photo irradiation effects on the bias current.

Linearly polarized laser light at 900 nm was focused onto the central part of one surface of the crystal. It has been known that metallic tubes in this system show strong absorption at 900 nm in E//C configuration, where E and C are the electric field vector of the laser light and the C-axis of the crystal or the tube axis, respectively. Before laser light irradiation, the I-V characteristics show ohmic nature as Tang et al. have reported [1]. After strong photo-irradiation with E//C, however, the bias current was dramatically decreased and showed slight deviation from the ohmic character in the I-V characteristics.

Plotted in Fig.2 is the deviation from the ohmic behavior by subtracting the ohmic part around zero-bias region from measured bias current, (a) before and (b) after the laser light irradiation. The ohmic character is seen in curve (a). On the other hand, the deviation was found to start at V = ± 0.25V in curve (b). The inset shows the first-order derivative of curve (b) in terms of V, to show the on-set voltage more clearly. The character is somewhat semiconducting.

We can speculate the following scenario to understand the mechanism of the change. The resultant current in the photo-irradiated sample can be due to remaining un-photo-modulated metallic tubes and the photo-modulated semiconducting ones. The on-set energy observed above suggests that the relevant band gap energy would be about

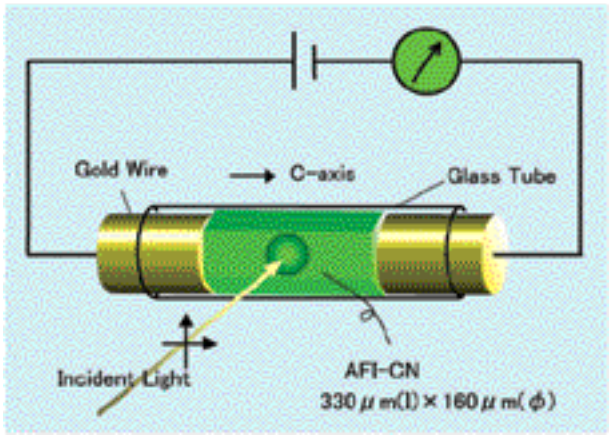

Fig.1. Experimental setup. A single AFI-CN crystal was inserted into a glass tube, and was pinched by two gold wires from both openings. Bias voltage was applied to CNs between these two wires.

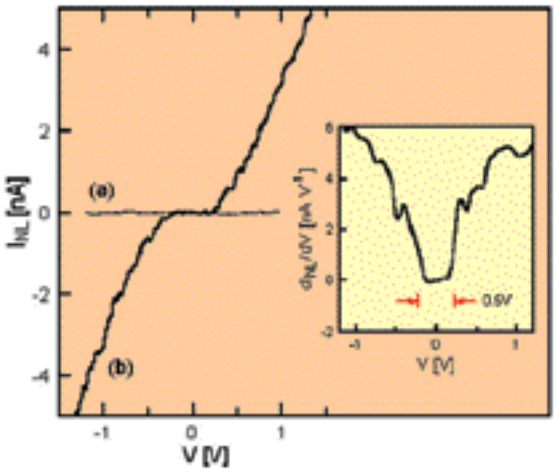

Fig. 2. Deviation from ohmic behavior of the bias current, (a) before and (b) after the photo-irradiation. Inset: The first-order derivative of curve (b).

0.5 eV. This value is not so unrealistic considering the accuracy of the band gap energies of relevant CNs predicted from the LDA calculation.

These results may suggest the potential application of CNs to novel opto-electronic devices.

References

[1] Z.K. Tang, H.D. Sun, J. Wang, J. Chen, and G. Li,Appl. Phys. Lett., **73** (1998) 2287.
[2] Z.K. Tang *et al*., Science, **292** (2001) 2462.
[3] Z.M. Li *et al*., Phys. Rev. Lett., **87** (2001) 12740.
[4] A. Jorio *et al*., Chem. Phys. Lett., **351** (2002) 27.
[5] Y. Kamada, N. Naka, and N. Nagasawa, Z.M. Li, and Z.K. Tang, Physica B, in press.

Authors

Y. Kamada[a], N. Naka[a], and N. Nagasawa[a], T. Suemoto and S. Saito
[a]Department of Physics, University of Tokyo

Synthesis of Large Single-Crystal Forsterite using CZ Method

K. Ito and T. Kitazawa

Forsterite is the most abundant phase of the Earth's mantle. Synthesis of high-quality large forsterite single crystals is essential to understand physical properties of the mantle. To study anisotropies in seismic velocity, elasticity, anelasticity, viscoelasticity, rheology, electrical conductivity, and thermal property, it is essential to determine the properties of mantle minerals along various crystallographic directions. For systematic anisotropy measurements, it is important to prepare homogeneous specimens cut for various crystallographic directions from one large single crystal. We report synthesis of large high-quality forsterite single crystals for use in physical property measurements at high pressure and temperature. We synthesized olivine single crystals by the CZ method with a pure-iridium crucible. A wide furnace space of the new CZ apparatus used in this study allows to mount a large Ir-crucible to ~90 mm diameter and ~90 mm height. The CZ apparatus is equipped with the automatic diameter control (ADC) system, which automatically maintains uniform crystal diameter. We will show as-grown crystals of forsterite and olivine. Figner 1 shows typical as-grown crystals of forsterite growing along the [100] direction. Careful preparations (weighing and mixing) of starting reagents enable us to create a high-quality crack-free forsterite specimen as shown in Fig. 1. In this sample, no inclusions, voids or defects are observed under stereoscopic

Fig.1. As-grown forsterite single crystals growing along the [100] direction. The unit of the measure is cm. The crystal has no cracks, inclusions or defects. A high-quality crack-free specimen is synthesized by using high-purity MgO and SiO_2 reagents.

microscope, except for facet. A thick long crystal can be produced by using a large volume crucible. Owing to the new ADC system, the present crystals have uniform diameter, and their cross sections are nearly perfect circle. Ultimately, we will be capable of producing specimen size to over 50 mm diameter and to ~250 mm length, by using a crucible of ~90 mm diameter and ~90 mm height. Large high-quality single crystals will be successively supplied for use in property measurements and laboratory experiments.

References

The author thanks the Material Design and Characterization Laboratory of the Institute for Solid State Physics of the University of Tokyo for the CZ facilities. This work was supported by grants from the Earthquake Research Institute of the University of Tokyo (2001-A-18).

Authors
K. Ito[a], H. Sato[b], H. Kanazawa[c], N. Kawame[c] and T. Kitazawa
[a]Faculty of Business Administration, Southern Osaka University.
[b]Department of Earth and Space Science, Osaka University.
[c]Department of Environmental Conservation and Development, Kyoto University.

Non-stoichiometry and Phase Transition of $EuBaCo_2O_{5+x}$ Double Perovskit —A TEM Study—

N. Nakayama and Y. Ueda

The transition metal oxides ABO_3 with perovskite-type structure exhibit a variety of interesting physical properties such as the colossal negative magnetoresistance of Manganites. The flexibility of perovskite-type structure, the accomodation of cations with the different ionic charge in A sites and/or the oxygen deficiency, stabilizes the wide range of valence state for transition metals in B sites and leads to the rich variety of the physical properties. The perovskite-type cobaltate is another candidate of the colossal negative magnetoresistant materials.

Recently, a series of cobaltate, $R BaCo_2O_{5+x}$ (R; rare earth metals), showing fairly high magneto-resistance has been found [1]. In these compounds, R and Ba atoms occupy the A-site in an ordered manner along c-axis. The crystal structure can be described as a layered arrangement of $RO/CoO_2/BaO/CoO_2$. The oxygen deficiency, (1-x) in

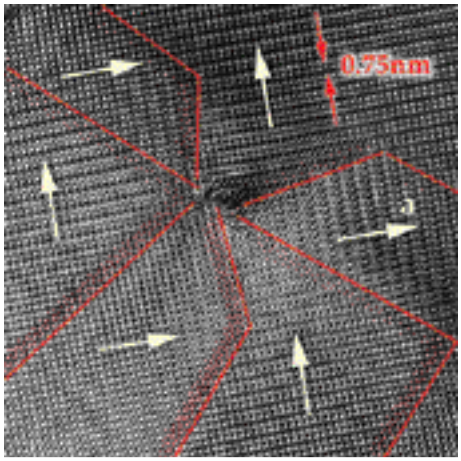

Fig.1 A high-resolution lattice image of $EuBaCo_2O_{5.25}$ viewed along the [001] direction. The oxygen non-stoichiometry is accommodated by the microdomain formation. Red lines indicate domain boundaries between the vacancy ordered regions.

$R BaCo_2O_{5+x}$, ranges from 0 to 1 ideally and oxygen vacancies are located at the RO planes. Oxygen vacancy orderings in the RO planes are reported for the compositions x = 0.5 and 0.43. The formal valence of Co atoms ranges from 3.5 to 2.5. At the specific compositions of x = 0 and 0.5, a charge order transition and a metal-insulator transition are reported, respectively. The oxygen non-stoichiometry has a crucial role on the physical properties of $R BaCo_2O_{5+x}$. However, no detailed study has been reported except for $YBaCo_2O_{5+x}$ system [2].

We have investigated $EuBaCo_2O_{5+x}$ system containing the larger R atoms and the results were compared with $YBaCo_2O_{5+x}$ system. The studies were focused on the direct observation of oxygen vacancy ordering by high-resolution TEM images and the TEM characterization of the low temperature charge ordered state.

Samples were prepared by the conventional ceramic method. After calcinations of starting mixtures at 1050°C, samples were annealed at several temperatures in O_2, N_2 or Ar stream to obtain samples with wide range compositions. The oxygen content was determined by TG-analysis in H_2. For $0.05 < x < 0.25$, the orthorhombic phase with the fundamental 112 structure (Pmmm, $a \approx b \approx a_0$, $c \approx 2a_0$) was

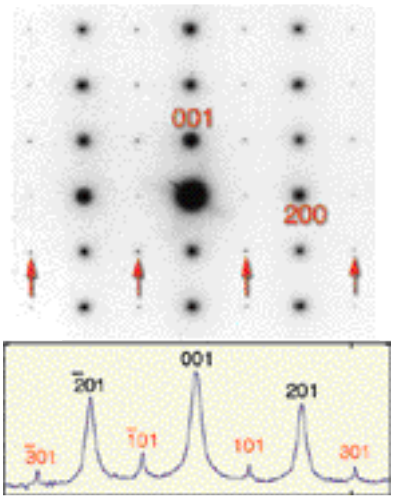

Fig.2. A [010]-zone electron diffraction pattern of the charge ordered state for $EuBaCo_2O_{5.05}$ below 200 K. The reciprocal lattice reconstructed from several ED patterns with different zone axes indicates the *Pmma* symmetry of the ordered state, which agrees with the stripe-type ordering model of Co(II) and Co(III).

obtained. Whereas for $0.25 < x < 0.65$, the orthorhombic phase with doubled *a*-axis due to the oxygen vacancy ordering was obtained. The $3a_0 \times 3a_0$ ordered tetragonal phase as reported for $ABaCo_2O_{5+x}$ with smaller A cations (Y, Ho etc) was not observed. The oxygen non-stoichiometry is accommodated by the micro-domain formation (Fig.1).

For the sample with $x = 0.05$, a charge order phase transition was found. DSC curves show two peaks at 250 and 360 K, corresponding to the charge order and the antiferromagnetic order, respectively. The magnetic susceptibility shows the anomalies at the transition temperatures.

Electron diffraction patterns at low temperatures indicate the doubling of *a*-axis due to the charge order (Fig.2). The extinction condition agrees with the symmetry of charge ordered phase (*Pmma*) of Y or Ho systems. Transition temperatures are 20-30 K higher than Y and Ho system as a result of volume effect.

References

[1] A. Maignan, C. Martin, D. Pelloquin, N. Nygyen, and B. Raveau, J. Solid State Chem. **142** (1999) 247

[2] D. Akahoshi and Y. Ueda, J. Solid State Chem. **156** (2001) 355

Authors

N. Nakayama[a], Y. Kubota[a], T. Mizota[a], and Y. Ueda

[a]Faculty of Engineering Yamaguchi University

A New Macroscopically Degenerate Ground State in the Spin Ice Compound $Dy_2Ti_2O_7$ under Magnetic Field

K. Matsuhira, Z. Hiroi and T. Sakakibara

Geometrical frustration can lead to novel phenomena such as a macroscopic degeneracy in the ground state with no long-range ordering. Recently, a new class of magnetic state known as “spin ice” (Figure 1) is discovered in the pyrochlore rare-earth [1].

In the pyrochlore lattice, a ferromagnetic interaction stabilizes the local spin arrangement of two spins pointing outward and two spins inwards (so-called ‘two-in two-out’ state) in a basic tetrahedron when there is a strong single-site anisotropy along the local <111> axes. For every tetrahedron, there are six possible combinations of spins under the two-in two-out rule reflecting the global cubic symmetry. In fact, the typical compound $Dy_2Ti_2O_7$ show the residual ground state entropy of 1.68 J/mol K, which is numerically in agreement with the Pauling's entropy for water ice [2].

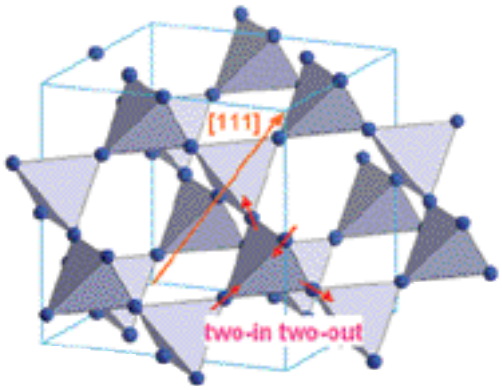

Fig. 1. Pyrochlore lattice of the corner-sharing tetrahedra whose vertices are occupied by Ising spins of Dy ions. The long arrow shows the [111] direction along which the magnetic field is applied. One of the six “two-in, two-out” configurations is shown by short arrows. Each spin lies along the axis joining the vertex and the center of the tetrahedron, due to a strong single-site anisotropy. Pyrochlore lattice can be viewed as an alternating stacking of kagomé layers and sparse triangular layers, both of which are perpendicular to the [111] direction.

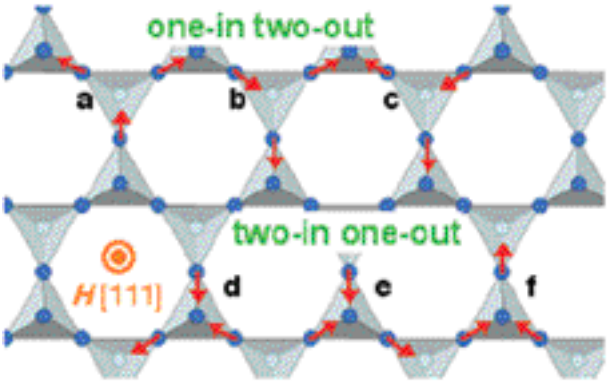

Fig. 2. Macroscopic degeneracy in the plateau state (kagomé ice). Here, **a**, **b** and **c** show the three patterns for the one-in two-out configurations for triangles with another apical spins above, whereas **d**, **e** and **f** are those for two-in one-out arrangements for the othertriangles with another apical spins below in the kagomé layer.

By applying magnetic field along the [111] direction, we found a new macroscopically degenerate ground state. Below 1 K, we observed a clear plateau in the magnetization process. The emergence of the plateau is closely associated with a formation of the spin ice state. The magnetic moment of the plateau is very close to the value expected for the satu rated moment along the [111] direction without destroying two-in two-out state. From the result of the field dependence of magnetic entropy at 0.4 K, we found that the plateau state is disordered with the residual entropy of nearly half the value of the zero-field state. The macroscopic degeneracy comes from a frustration of the spins on the kagomé layers perpendicular to the magnetic field. The magnetic field along the [111] direction reduces the sixfold degenerate two-in two-out configurations in the basic tetrahedron to threefold. In this state, every spin on the triangular layer is oriented along the [111] direction whereas the spins on the kagomé layer are still frustrated because the two-in two-out ice rule is maintained in each tetrahedron. The kagomé layer consists of corner-shared triangles, and under the ice rule, there are two types of triangles having the spin configurations of either one-in two-out or two-in one-out (Figure 2). For each type, there are three ways to align the spins. Our experimental data confirm this new macroscopically degenerate state (‘kagomé ice’ state) in $Dy_2Ti_2O_7$ under magnetic fields.

References

[1] M.J. Harris *et al*., Phys. Rev. Lett. **79** (1997) 2554.

[2] A.P. Ramirez *et al*., Nature **399** (1999) 333.

Authors

K. Matsuhira[a], Z. Hiroi, T. Tayama, S. Takagi[a] and T. Sakakibara.

[a]Kyushu Institute of Technology

Order-Disorder Transition in Cubic Cd_6M and its Low Temperature phase

R. Tamura and Y. Ueda

Recently, a new class of the icosahedral (i) quasicrystal (QC) was found as a stable phase in Cd-Yb and Cd-Ca alloys[1], which are the first binary stable iQCs to be identi-

fied. After the discovery, Takakura *et al.*[2] pointed out that cubic Cd_6Yb and Cd_6Ca crystals are the 1/1 cubic approximants of the Cd-Yb and Cd-Ca QCs. Cd_6Yb is reported to have space group of *Im*3, which contains 168 atoms in a unit cell with a = 15.638 Å.The structure can be described as *bcc* packing of an icosahedral cluster composed of 66 atoms. Interestingly, the core of the icosahedral cluster is an atomic shell of non-icosahedral symmetry, four Cd atoms reside at the vertices of a small cube with half occupancy forming a tetrahedron. In the course of our systematic investigation of the transport behavior in the binary QCs and their approximants[3], we found the occurrence of an order-disorder phase transition at about 110 K and 100 K in the Cd_6Yb and Cd_6Ca cubic crystals, respectively, as described below[4.]

The resistivity of the Cd_6Yb and Cd_6Ca cubic crystals show a stepwise change at 110 K and 100 K with a discontinuous change of TCR(temperature coefficient of the resistivity) across the step. No hysteresis is observed in the resistivity change for decreasing and increasing cycles of the temperature. Results of the specific heat measurements also exhibit a small peak at about 110 K and 100 K, respectively. The fact that these temperatures correspond precisely to the temperatures of the resistivity jump verifies the occurrence of a phase transition at these temperatures. On the other hand, no discontinuous shift was evident from powder X-ray diffraction spectra at temperatures above and below 110 K for Cd_6Yb. However, slight peak-broadening has been observed at 110 K, which occurs reversibly when the temperature cycle is repeated. This result is taken as indication that the phase transition at 110 K accompanies the introduction of some kind of disorder.

As shown in Fig.1, we clearly observe a change of the electron diffraction pattern below and above 110 K for Cd_6Yb. The figure shows the patterns obtained for the same grain at 130 K(a) and 14 K(b) for Cd_6Yb. Pattern (a) shows a diffraction pattern taken along [013] and is indexed as given in the figure, satisfying the extinction rule of the *bcc* structure, which is consistent with the reported space group *Im*3 for Cd_6Yb. Meanwhile, in pattern (b), additional weak spots appear in a commensurate manner to pattern (a). These spots are regarded as the superlattice spots due to the ordering of the structure. We confirmed that the change of the diffraction pattern is reversible for the temperature cycle and thus it indicates that the phase transition is an order-disorder

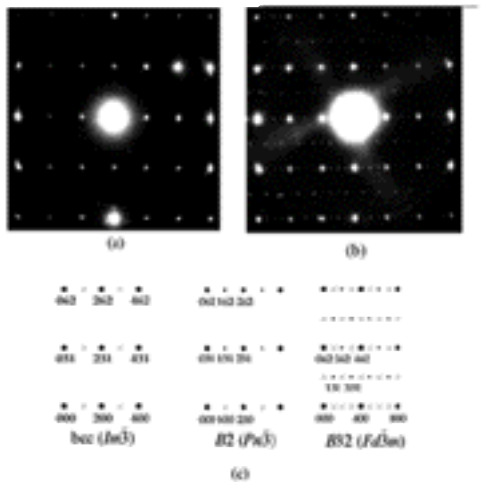

Fig.1. Electron diffraction patterns of Cd_6Yb taken along [013] at 130 K (a) and at 14 K (b). Electron diffraction patterns expected from the *bcc*, the ordered *B*2 and the ordered *B*32 structures (c).

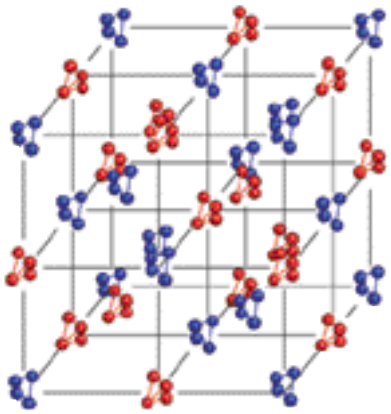

Fig.2. Schematic illustration of the *B*32 ordered arrangement of the central 4Cd tetrahedral. The 4Cd tetrahedra of different orientations are indicated by different colors.

transition. Close examination of diffraction patterns of the ordered phase has revealed that the superlattice spots are mostly described as *F*-type reflections from a superstructure of double unit cell. Considering that the transition is most probably due to the orientational ordering of tetrahedral 4Cd clusters sitting at the center of dodecahedral cages, we are led to a conjecture that above 110 K (100 K) the central 4Cd cluster is disordered over two orientations resulting in a *bcc* structure (*Im*3), whereas below 110 K, it is ordered in *F*-type superstructure (*B*32) (c).

Figure 2 illustrates schematically the *B*32 ordered arrangement of the central tetrahedra. Such *B*32 ordering is plausible since the point symmetry of the nearest icosahedral cluster arrangement is the same as that of the central 4Cd cluster, which would result in reduction of the strain energy.

References

[1] A.P. Tsai *et al.*, Nature **408** 537(2000) .
[2] H. Takakura *et al.*, Philos. Mag. Lett. **81** 411(2001) .
[3] R. Tamura *et al.*, Jpn. J. Appl. Phys. **40** L912(2001) .
[4] R. Tamura *et al.*, Jpn. J. Appl. Phys. **41** L5242002) .

Authors

R. Tamura[a], Y. Murao[a], S. Takeuchi[a], M. Ichihara, M. Isobe and Y. Ueda

[a]Department of Materials Science and Technology, Science Univesity of Tokyo

High Pressure X-ray Study on Organic Charge Transfer Salts

H. Sawa and J. Yamaura

It is well known for many organic charge transfer salts that the applying pressure induces a various changes of physical properties. It is significant that the crystal structure determination under pressure to discuss the origin of the high-pressure state. We have been developing the X-ray study under pressure at the X-ray laboratory in the material design and characterization laboratory.

β'-Pd(dmit)$_2$ anion radical salt is characterized by a solid-crossing columns composed by strongly dimerized $Pd(dmit)_2$ units. This is a unique two-band system associated with two-dimensional HOMO-based band and one-dimensional LUMO-based band [1]. Several compounds show metallic and superconducting states under pressure which are followed by a non-metallic state under higher pressure region. X-ray single crystal structure analysis was

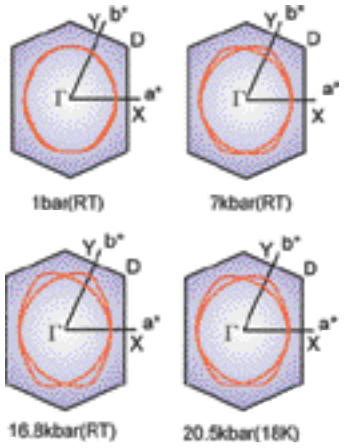

Fig. 1. Fermi surface of the HOMO band under pressure at room and low temperatues. They are multiple ones due to solid-crossing columns. Lowering the dimensionality under pressure is related to the non-metallic state in the higher-pressure region.

carried out for the high-pressure superconductor β-$Et_2Me_2P[Pd(dmit)_2]_2$ (T_c = 4 K at 7 kbar) under pressure at room temperature and low temperature to clarify the nature of the electronic states. The diffraction data under pressure were collected using an imaging plate type Weissenberg camera equipped with a diamond anvil cell (DAC). We calculated the band parameters based on the extended Hückel method from the refined crystal structure under pressure, indicating an increase of bandwidth and a decrease of the dimensionality of a HOMO-based band. Figure 1 shows the calculated Fermi surface of the HOMO band, which means the decrease of dimensionality under pressure. The above findings are related to a pressure-induced metallic state and a non-metallic state in the higher-pressure region.

(R_1,R_2-DCNQI)$_2$Cu salts have a 1D column structure of DCNQI molecules, where the column networks are bridged by Cu ions. They exhibit various unique physical properties due to the hybridization between 1D organic DCNQI pπŒ-band and Cu d_{xy}-orbitals near the Fermi level [2]. Among them, we are interested in the $R_1 = R_2$ = I (DI) and $R_1 = R_2$ = Br (DBr) salts having the complicated pressure-temperature phase diagram, that is, the ground state changes successively under pressure as metal(M_I) → insulator(I_I) → metal(M_{II}) → insulator(I_{II}) → metal(M_{III}). In order to identify the origin of the complicated phase diagram, we measured the X-ray diffraction of the powder samples under pressure for DI and DBr salts using a special designed powder type DAC. We found the different pressure dependence in the lattice parameter (Fig. 2), estimated by the Rietvelt method, for each salt. This suggests that the electronic state under pressure is different between them although they have similar conductive properties under pressure.

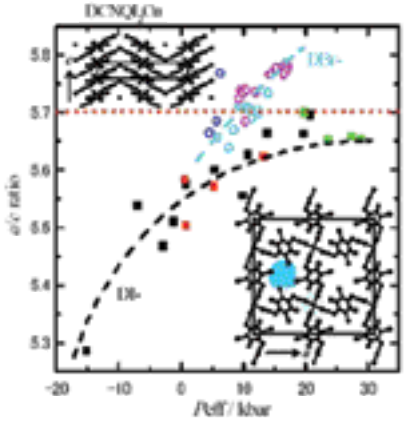

Fig. 2. Pressure dependence of the lattice parameter ratio of *a*/*c* for DBr and DI salts with the crystal stucture of (R_1,R_2-DCNQI)$_2$Cu. They show the different dependence of their values in higher-pressure region. The pressure value is normalized by the critical pressure for each salt.

References
[1] R. Kato, Y-L. Liu, Y. Hosokoshi, S. Aonuma and H. Sawa, Mol. Cryst. Liq. Cryst. **296**, 217 (1997).
[2] R. Kato, H. Kobayashi and A. Kobayashi, J. Am. Chem. Soc. 111, 5224 (1989).

Authors
J. Yamaura and H. Sawa[a]
[a]KEK (Japan)

Dynamics of an Isolated Twin Boundary

K. Kawabata and H. Takayama

In the ISSP collaboration with theory groups (Matukawa, Nemoto, Takayama) and experimental groups (Kawabata, Sambongi), we discussed dynamics of an isolated twin boundary in order to clarify the mechanism of its mobility. Charge transfer complex $(TMTSF)_2X$ has triclinic crystallographic structure. TMTSF and X denote tetramethyl-tetraselena-fulvalene and an anion such as PF_6^+, respectively. Planer TMTSF molecules are stacked along needle axis. The twin boundary is formed in a single crystal of $(TMTSF)_2X$ when the stress is applied in a suitable manner. The boundary can move easily under a weak shear stress. It is quite unique that the boundary is visible as a kink of the needle shape crystal as shown in Fig.1-a.

Then its position can be measured definitely by optical microscope and a digital recorder in real time. An isolated boundary was forced to move repeatedly under constant stress within the same area of the crystal. The motion of the boundary was found unusual, as follows. The boundary moves intermittently; it stops at some positions and moves again after intermission ranging over tens of seconds even under constant external stress. We considered that the intermission occurs at some strong pinning centers like defects and/or impurities and that many internal degrees of freedom existing in the present system are essential. We found that the mobility of the boundary is affected strongly by the

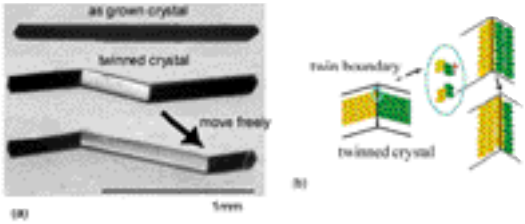

Fig. 1. (a) A single crystal of $(TMTSF)_2X$ before and after twin deformation. The twin boundary appears as a kink in morphology, which reflects to its twinned crystal structure. (b) Schematic model for twin boundary motion. When the boundary moves ahead in lattice spacing, molecules on one side of the boundary slide along lattice array on the other side. The twin boundary motion is in a similar situation to dry friction between two commensurate lattices.

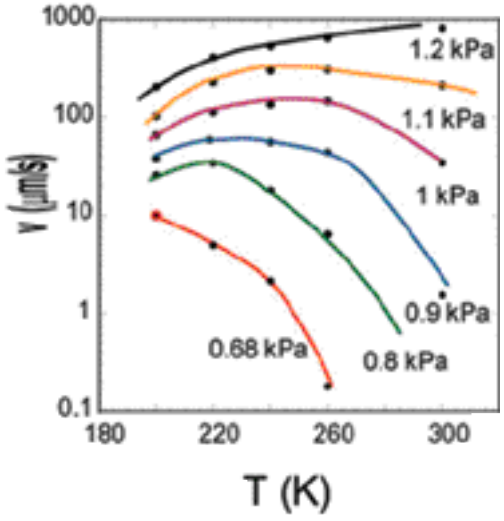

Fig. 2. Temperature dependences of the local velocity for various external stresses. When the temperature is lowered, the velocity decreases under the external stress of 1.2 kPa, while the velocity increases under 0.68 kPa.

waiting time, which corresponds to the time elapsed before the boundary passes forward through each position after the backward passage. The velocity becomes lower as the waiting time is longer [1]. We succeeded in proposing a model that the imperfections, which created by the backward motion and recovered for the waiting time, assist the mobility of the boundary.

On the other hand, we focused that the twin boundary motion is in a similar situation to dry friction of solid on solid systems. In the case that a unit cell is simple, each molecule on one side of the boundary slides over molecule array of the other side for lattice spacing along the twin boundary plane, when the boundary goes ahead for lattice spacing, as shown in Fig.1-b. Then, the twin boundary motion can be considered as an elementary process of dry friction between two commensurate lattices without wearing. We found similarity of the motion between the twin boundary and frictional sliding of a paper on paper system, which was previously reported by Heslot et al [2]. The present system is useful to examine temperature effects on the friction phenomena, since it is difficult to carry out friction experiments of solid on solid systems at various temperatures. We found that the obtained temperature dependence is complicated, as shown in Fig. 2 [3].

When the temperature is lowered, the velocity decreases with the stress under 1.2 kPa, while the velocity increases under 0.68 kPa. Taking into consideration of the temperature dependent threshold stress σ_c, the obtained results were replotted as a function of temperature under constant effective stress, which is defined as $\sigma - \sigma_c$. The temperature dependence can be represented well as a thermal activation type. The activation energy was estimated as about 0.1 eV and almost independent of the effective stress. This implies that the boundary motion includes some nucleation process.

References

1. M. Mukoujima, K. Kawabata, T. Sambongi, Eur. Phys. J. **B7**, 365-369 (1999).
2. F. Heslot, T. Baumberger, B. Perrin, B. Caroli, and C. Caroli, Phys. Rev. **E49** (1994) 4973.
3. K. Kawabata, Y. Hosokawa, T. Kawauchi and T. Sambongi, Ferroelectrics, **251**, 199-205 (2001).

Authors

K. Kawabata[a], H. Takayama, H. Matukawa[b], K. Nemoto[a], T. Sambongi[c]
[a]Hokkaido University., [b]Osaka University., [c]Hokkaido Information University.

ISSP WorkShop (April 2001～March 2002)

1. Chemistry and physics of oxides with 3D geometrical frustration

May 31~June 1, 2001

Geometrical frustration among localized spins is known to cause anomalous ground state degeneracy and fluctuation effects. Recent extensive studies on pyrochlore and spinel oxides have revealed rich variety of anomalous phenomena not only for insulating spin system but for itinerant electron systems. In this workshop, the latest experimental and theoretical results on these oxides were presented.

2. Chemistry of transition metal oxides: Present status and future of materials search for novel physics and applications

June 18~20,2001

The remarkable discovery of high-Tc superconductivity and the following enthusiastic research in the last decade have clearly exemplified how the finding of new materials would give a great impact on the progress of solid state physics and its application to technology. Now the related topics are spreading over not only superconductivity but also an unusual metallic behavior which is generally seen near the metal-insulator transition in the strongly correlated electron system. We believe that for the next few decades it will become more important to explore novel physics through searching for new materials. Transition-metal oxides are one of the most typical system where the effect of Coulomb interaction plays a critical role on their magnetic and electronic properties. Especially interesting is what is expected when electrons localized due to the strong Coulomb repulsion start moving by changing the band width or the number of carriers. We anticipate there an unknown, dramatic phenomenon governed by quantum fluctuations. In this meeting specialists from various areas of research got together to discuss the general idea on materials research.

3. New developments of charge ordering phenomena

June 27, 2001

Recently charge ordering phenomena have been discovered in many materials, including manganese, cobalt and vanadium oxides and organic charge transfer salts. This one-day workshop was organized to discuss these phenomena, in particular the behavior under high pressure and magnetic field, as well as the related theoretical models.

4. Superfluidity and quantum vortex in quantum condensed system : Superfluid He and Bose-Einstein condensation (BEC) in neutral atomic gases

October18~19,2001

It is not too much to say a BEC in a laser-cooled alkali atomic gases is one of the most active field in condensed matter physics. The concepts of a condensate, an elementary excitation and a quantum vortex etc. in BEC in gas strongly reflects those of superfluid He in a conventional low temperature phsics. In Europe and U.S.A., there exists a close communication among those who work in quantum electronics and low temperature physics, resulting into promoting the reseach in the " quantum coherent system " in both fields. On the other hand, in our country, there was no such communication at all, which is an unfortunate situation. Recenkly we started some actions to improve the situation, and the present meeting is also one of such activities. Just before this meeting, this year's Nobel prize in physics was annonced to be awarded for the realization and basic research in BEC in dilute alkali atomic gases. As a result of heated atomosphere in related communities, we had about eighty participants and lively discussions among them. We are very happy if this meeting gives a good chance to cause a rapid progress in the research field of " quantum coherent system " in our country.

5. High magnetic fields: Physics and technology

November 5 ~ 16, 2001

Recently, high magnetic field science has attracted much attention, and a number of new large facilities for high magnetic fields have been built in the world. Many novel interesting results have been obtained using the high magnetic fields. It has long been argued in Japan, that a new collaborative scheme is necessary among the research groups who are working on the physics in high magnetic fields in Japan, in order to stimulate the activity in this research area and to strengthening cooperation among the groups. It has been agreed that the High Magnetic Forum Japan should be established in autumn 2002, and that a seminar should be organized at least once a year to discuss about the latest results and the future collaboration. This Workshop was organized as the first meeting of this kind. A variety of topics have been discussed in the two-days workshop. In particular, a focus was put on new techniques for generating high magnetic fields and for precise data acquisition in the high fields. A new direction of the research was also discussed.

6. Applications of new light sources and future prospect

November 19 ~ 20, 2001

Recently the brightness of synchrotoron radiation (SR) has been improved and long undulators are becoming light sources with spatial coherence as high as lasers. New coherent light sources such as high-order harmonics at the soft X-ray region, free electron lasers at the farinfrared region and terahertz radiation by femtosecond lasers have appeared on the stage. Furthermore the slicing of femtosecond pulses from SR by lasers is becoming to an application level. On the other hand, in the field of dynamics in structure and phase transition, some interesting demonstrations like time-resolved X-ray diffraction are reported. In this symposium, researchers concerning with the development of light sources, spectroscopy and theory gathered to discuss about new achievement, present status and future plan on researches by new light sources and spectroscopic methods at the visible and infrared regions.

7. Unconventional superconductivity in the heavy-electron compounds $CeTIn_5$

December 7 ~ 8, 2001

The heavy-electron compounds UGe_2 and $CeTIn_5$ (T = Co, Ir, Rh) have been attracting considerable interest, because of their unusual superconducting properties. UGe_2 is a ferromagnet at an ambient pressure, and under the pressure of ~ 1 GPa exhibits a superconducting transition that is considered to be coexisting with ferromagnetism. While $CeRhIn_5$ is an antiferromagnet, $CeCoIn_5$ becomes an ambient pressure superconductor with the highest known transition temperature (2.3 K) for any heavy-electron systems. The $CeTIn_5$ compounds are therefore considered to present an uncommon opportunity to study the interplay of superconductivity and magnetism in heavy-electron systems. Recent activities on these topics are presented as 27 talks and discussed in this workshop. troscopic methods at the visible and infrared regions.

8. Physics of Vortex Matter in High temperature Superconductors.

December 10 ~

The purpose of this conference is to clarify (1)the static and dynamic phase diagram of the "composite vortex matter", which is realized in highly anisotropic high temperature superconductors in magnetic field, (2) the electronic structure in the vortex state of unconventional superconductors, and (3) the feasibility of device application of the vortices. In the vortex matter, various kinds of ground states are realized by the interaction, thermal fluctuation, and randomness. Moreover the electronic state of the two dimensional vortices is not well known. In the conference, the above topics were discussed in 45 talks by 65 participants.

9. Meeting on $Cd_2Re_2O_7$.

January 30, 2002

Since $Cd_2Re_2O_7$ was discovered to be the first superconductor among the the pyrochlore oxides at ISSP, active research has been pursued. In this workshop, the latest results on the superconducting and other physical properties of this material were intensively discussed. In particular, the nature of the successive structural transitions and the changes of physical properties caused by them were the target of active discussion that revealed anomalous character of itinerant electron systems on a pyrochlore lattice.

10. Structural fluctuation of Si(100) surface

February 1, 2002

Surface atoms on Si(100) are reconstructed to form a (2x1) dimer row structure. Many experimental and theoretical studies have supported the buckled (asymmetric) dimer with c(4x2) phase as a ground state, although some quantum chemical studies including electron correlation have proposed a symmetric dimer as the most stable state. Recently, several low temperature STM studies have reported symmetric dimer images. With decreasing the substrate temperature from 80 K to 5 K, the area of symmetric dimer image increases. However, the origin of such symmetric images is a controversial issue (dynamic or static). In this workshop, we have discussed the surface structure of Si(100) at low temperature. Recent low temperature STM studies have been presented as well as other experimental investigations including surface diffraction, surface phonon spectroscopy, high resolution core-level photoelectron spectroscopy and theoretical studies. More than fifty researchers and graduate students participated in this workshop and discussed this controversial issue in detail.

11. Recent developments in quantum Hall systems

February 15~16,2002

The quantum Hall systems, i.e. two-dimensional electron systems in semiconductor heterostructures in strong magnetic fields and low temperatures, are well established as a highly controled experimental stage of the physics of strong correlation. Recently, there are a few new developments in this field, including, interlayer coherence in double layer quantum Hall systems, stripe phase (charge density wave phase) in higher order Landau levels, long relaxation phenomena involving nuclear spins, edge states and chiral surface states in multilayer quantum Hall systems, etc. Together with Professor Z.F.Ezawa, who is a Visiting Professor of ISSP this year, we made a plan for a workshop in which a relatively small number of experimentalists and theorists have a intensive discussions on these and related topics. The proposal for such a workshop has been granted as a ISSP Workshop, and the Workshop was held in February 15th (Fri.) and 16th (Sat.) in the Lecture Hall of ISSP. The Workshop turned out to be very successful with about 40 researchers and students participating in active discussions on such subjects as, (1)the many body states of the quantum Hall systems with extra degrees of freedom, (2)the relation between the stripe phase and externally applied potential modulation, (3)the mechanism of the breakdown of quantum Hall states, (4)transport phenomena in antidot and multilayer systemsprogress in the research field of " quantum coherent system " in our country.

12. New Synchrotron Light Source in Japan

February 22~23,2002

The symposium attracted over 80 scientists in the field of accelerator, solid state and soft materials science, had 18 invited presentations on the application of undulator radiation, and had two group discussions. The organizers were Professors S. Sato (Tohoku University), H. Fukuyama (The University of Tokyo, ISSP) and Y. Kimura (KEK, IMSS), who had been discussing on the future plan of the synchrotron radiation facility in Japan. In opening the symposium, Dr. N. Kumagai (SPring-8) reported on the discussion at the light source design working group and showed a new 1.6-1.8 GeV electron storage ring with 10 insertion devices optimised in EUV and SX region. The design and the applicability of the new light source were discussed keenly throughout the two-days symposium from both viewpoints of synchrotron radiation users and accelerator scientists. The results of the symposium were applied to modify the design, and the construction plan of a 1.8 GeV electron storage ring with 12 insertion devices was proposed as the future synchrotron light source in Japan.

13. ISSP Theory forum for the 21st century.

March 7~8, 2002

Discovery of new materials and development of nano-structure and soft-materials have made condensed matter theory even more exciting and challenging. At the same time, however, one tends to focus on specialized problems and communications among researches working on different disciplines are becoming increasingly difficult. This workshop is organized to provide opportunities for young condensed matter theorists to discuss new concepts and methods common to many sub-fields of condensed matter physics across different disciplines. The program included 30 minutes review talks intended to serve for non-specialists and poster sessions from general contributors, as well as a few keynote speech from experimentalists that provided new theoretical problems. The workshop was very successful with active discussions among more than 90 participants.

14. Proposal of the monochromator and the characterization of the optical elements for the VUV-SX high brilliant light source beamlines

March 19, 2002

The high brilliant light source project around the extreme ultraviolet(EUV) and the soft-X ray (SX) region is now discussed and designed as a national project. The members of the working group for the accelerator, the beamlines and the research field are selected from many facilities, institutes and universities in Japan. In order to proceed the design of the monochromator suitable for the high brilliant light source with highperformance, i.e., high energy resolution, high photon flux, small spot sizeetc, the R&D's to develop the optical elements such as multilayer mirrors, zone plate, grating and so on are very important. In this workshop, the present status of the characterization of optical elements are discussed. The proposal and the demand to achieve the high performance beamlines are also discussed.